AWARD NUMBER: W81XWH-17-1-0525

TITLE: Iron Chelation Enhances TAM and Triple-Negative Breast Cancer Cell Death

PRINCIPAL INVESTIGATOR: Jason Koutcher

CONTRACTING ORGANIZATION: Sloan Kettering Institute for Cancer Research

REPORT DATE: OCTOBER 2021

TYPE OF REPORT: Annual Technical

PREPARED FOR: U.S. Army Medical Research and Development Command
Fort Detrick, Maryland 21702-5012

DISTRIBUTION STATEMENT: Approved for Public Release;
Distribution Unlimited

REPORT DOCUMENTATION PAGE

Form Approved
OMB No. 0704-0188

1. REPORT DATE	2. REPORT TYPE	3. DATES COVERED
OCTOBER 2021	Annual	9/15/2020- 9/14/2021

4. TITLE AND SUBTITLE

Iron Chelation Enhances TAM and Triple-Negative Breast Cancer Cell Death

5a. CONTRACT NUMBER

5b. GRANT NUMBER
W81XWH-17-1-0525

5c. PROGRAM ELEMENT NUMBER

6. AUTHOR(S)
Jason Koutcher (initiating PI) and Taha Merghoub (Partnering PI)

E-Mail: koutchej@mskcc.org ; merghout@mskcc.org

5d. PROJECT NUMBER

5e. TASK NUMBER

5f. WORK UNIT NUMBER

7. PERFORMING ORGANIZATION NAME(S) AND ADDRESS(ES)

Sloan Kettering Institute for Cancer Research
1275 York Avenue, New York, NY 10065-6007

8. PERFORMING ORGANIZATION REPORT NUMBER

9. SPONSORING / MONITORING AGENCY NAME(S) AND ADDRESS(ES)

U.S. Army Medical Research and Development Command
Fort Detrick, Maryland 21702-5012

10. SPONSOR/MONITOR'S ACRONYM(S)

11. SPONSOR/MONITOR'S REPORT NUMBER(S)

12. DISTRIBUTION / AVAILABILITY STATEMENT

Approved for Public Release; Distribution Unlimited

13. SUPPLEMENTARY NOTES

14. ABSTRACT The goal of this study is preclinical testing of Deferiprone (DFP), an iron chelator in clinical use for non-oncologic diseases. We completed in vitro testing proposed in the application. We found that DFP increased M1 polarization(even in the absence of IL4 or LPS) and also in the presence of LPS. DFP enhanced the efficiency of phagocytosis by RAW264.7 cells and was significant in all the culture conditions ($p = 0.0004$ for Control, $p = 0.0007$ for IL-4, $p = 0.0045$ for LPS) but most prominent in the LPS treated group. We measured the tumor cell doubling times including an additional cell line (BT474)and the effect of DFP and found the results similar in all 3 breast cancer cell lines. The IC50 values for the BT474 were similar to the 4T1 and MBA-231 cells. We previously reported the effect of DFP on oxygen metabolism and comsumption and extended these results by increasing the n value from n=3 →n=5

15. SUBJECT TERMS
Breast cancer, iron imaging, MRI, metabolism, cytokines, immune effects, deferiprone, CD4, CD8

16. SECURITY CLASSIFICATION OF:			17. LIMITATION OF ABSTRACT	18. NUMBER OF PAGES	19a. NAME OF RESPONSIBLE PERSON
a. REPORT	b. ABSTRACT	c. THIS PAGE			USAMRMC
Unclassified	Unclassified	Unclassified	Unclassified	39	19b. TELEPHONE NUMBER *(include area code)*

Standard Form 298 (Rev. 8-98)
Prescribed by ANSI Std. Z39.18

TABLE OF CONTENTS

1. **INTRODUCTION:** ***Narrative that briefly (one paragraph) describes the subject, purpose, and scope of the research.***

The goal of this study is preclinical testing of Deferiprone (DFP), an iron chelator in clinical use for nononcologic diseases. We propose to demonstrate the sensitivity of TNBC to DFP as a single agent, and in combination with immune modulation therapy (checkpoint inhibitors) and chemotherapy (paclitaxel and cisplatin). Studies were planned to be performed sequentially by first studying in vitro effects of DFP, followed by in vivo effects, and the effects of adding paclitaxel (taxol), cisplatin, and checkpoint inhibitors. We also measure the immune effects of DFP on cells (in vitro) and organs (ex vivo) including tumors.

2. **KEYWORDS:** *Provide a brief list of keywords (limit to 20 words).*

Breast cancer, iron imaging, MRI, metabolism, cytokines, immune effects, deferiprone, CD4, CD8

3. **ACCOMPLISHMENTS:** *The PI is reminded that the recipient organization is required to obtain prior written approval from the awarding agency grants official whenever there are significant changes in the project or its direction.*

What were the major goals of the project?

List the major goals of the project as stated in the approved SOW. If the application listed milestones/target dates for important activities or phases of the project, identify these dates and show actual completion dates or the percentage of completion.

Aim 1 Determine how inhibition of iron metabolism and OXPHOS impedes TAM function and metabolism, and reduces proliferation of macrophages and TNBC cells.

Aim 2: *Develop and validate non-invasive MRI methods to quantitatively and spatially monitor tumor and tissue iron and TAM infiltration, to detect changes induced by macrophage focused therapy*.

Aim 3: *Determine if inhibition of iron metabolism, TCA cycle, and OXPHOS by DFP: i) inhibits tumor growth, and ii) enhances responses to chemotherapy and immune checkpoint inhibitors in orthotopic TNBC*

What was accomplished under these goals?

For this reporting period describe: 1) major activities; 2) specific objectives; 3) significant results or key outcomes, including major findings, developments, or conclusions (both positive and negative); and/or 4) other achievements. Include a discussion of stated goals not met. Description shall include pertinent data and graphs in sufficient detail to explain any significant results achieved. A succinct description of the methodology used shall be provided. As the project progresses to completion, the emphasis in reporting in this section should shift from reporting activities to reporting accomplishments.

Aim 1 – We previously reported the effects of DFP on metabolism in the 4T1 and MDA-MB-231 TNBC cell lines. During previous years we completed 1) studies on the changes in MDA-MB-231 and 4T1 metabolism (**Koutcher Lab**) by DFP 2) found that this methodology did not work for studying macrophages. This year we implemented an alternate technique that will work to complement (as proposed) the tumor cell studies by doing them on macrophages. We measured changes in oxygen consumption induced by DFP in both tumor cells and macrophages and further extended these studies in the past year (**Merghoub and Koutcher Labs**), 3) the effect of DFP on macrophage and their immune function and phagocytosis (**Merghoub and Koutcher lab**). This has been the main focus of Year 4. Our preliminary in vivo studies (not reported this year – will be presented in final report) are disappointing; with the assent of Dr. Shuman-Moss we studied the doubling times and IC50 for the BT474 and began in vivo studies (Aim 3). These results summarized in detail on the attached sheets following this page.

The report is configured as 5 separate sub-reports, each written as an independent section. The references and figures are similarly numbered by section.

Section 1: Aim 1A: *Evaluate in vitro the effects of deferiprone (DFP) on tumor cell oxygen consumption rates (OCR), macrophage polarization, proliferation, and function.* (**Koutcher/Merghoub/Blasberg Laboratory**)

Data on macrophage proliferation was previously presented (2019). Data on macrophage OCR was presented in 2020 and is updated in the section on OCR below (section 5).

Effect of DFP on macrophage polarization

In this section, we have examined the effect of DFP on macrophage polarization from M0 to M1 and M2 cells upon exposure to lipopolysaccharide (LPS) and IL4 respectively in vitro. In the 2020 report, we provided immune response data from in vivo measurements focusing on T cells.

To examine the effects of DFP on macrophage polarization and effector function, we cultured RAW 264.7 cells in the presence of LPS (100 ng/ml) and murine IL-4 (10 ng/ml) for 48 hours to polarize these cells to M1 and M2 macrophages, respectively. We confirmed the polarization of RAW 264.7 cells by flow cytometry by examining CD206 and MHC class II expression. The macrophage cell line RAW264.7 (RAW) maintains an M0 phenotype (Control) when in culture, while the presence of IL-4 polarized these cells to a M2 phenotype (CD206+MHC II-) and LPS polarized them to a M1 phenotype (Fig. 1A). When DFP (100 μM) was added to the cultures, there was an increase in M1 polarization in the control conditions without IL-4 or LPS (control, from 3% to 7%, $p = 0.0016$) and also in the presence of LPS (from 26% to 37%, $p = 0.0016$) (Fig. 1B). However, we did not observe any effects on M2 polarization (Fig. 1B, left). Data are reported in this section as mean ± SD.

Studies on Macrophage Functional Response to DFP

To assess whether any of the phenotypic changes observed translated into functional changes in the RAW 264.7 cells, we tested their ability to 1) secrete cytokines, 2) phagocytose IgG-coated latex beads and 3) synthesize reactive oxygen species (ROS). We tested cell culture supernatants from RAW 264.7 cells that have been treated with IL-4, LPS (+/- DFP) for three cytokines (IL-10, IL-12, and TNFα) that are known to be associated with M1 or M2 macrophage polarization using the Luminex multiplex cytokine detection system (Millipore). While we were able to detect very small amounts of IL-12 in the supernatants from the cultures, their numbers were inconsistent between replicate experiments (data not shown). We found that RAW 264.7 cells polarized to M2 macrophages with IL-4 secrete more anti-inflammatory cytokines, such as IL-10 (Fig. 1C left), and less pro-inflammatory cytokines such TNFα (Fig. 1C, right). The addition of DFP to these cells appear to decrease both IL-10 and TNFα but this effect is subtle and was not observed in a second replicate experiment (data not shown). When RAW 264.7 cells were polarized to M1 macrophages with LPS, they secrete more pro-inflammatory cytokines such as TNFα (Fig. 1D). Unexpectedly, LPS also stimulated RAW 264.7 cells to secrete IL-10. This has been reported in the literature as a late phase response to LPS that may be a feedback mechanism to curtail the pro-inflammatory effects of LPS (1,2). While the addition of DFP did not enhance the secretion of TNFα, it did decrease the amount of IL-10 made in response to LPS by ~45% ($p = 0.0007$). Thus, DFP may negate the feedback mechanisms that are induced by LPS to promote a stronger pro-inflammatory response.

We tested the ability of RAW 264.7 cells, polarized with IL-4 and LPS, to phagocytose IgG-coated FITC-conjugated latex beads (via Fc-receptors). Unpolarized RAW cells had some baseline phagocytosis where ~18% of the cells phagocytosed latex beads (Fig. 2 A, B *Control*). Phagocytosis was not affected when cells were polarized to an M2 phenotype with IL4 (Fig. 2 A,B *IL-4*), however, phagocytosis was significantly enhanced (18% vs. 45% FITC+ cells, $p < 0.0001$) when cells are polarized to an M1 phenotype (Fig. 2 A,B *LPS*). The addition of DFP to these cultures has a subtle (with mixed statistical significance) increase in phagocytosis overall. While the effects of adding DFP were subtle with respect to the percentage of RAW 264.7 cells that have phagocytosed latex beads, DFP significantly enhanced the amount of latex beads that have been phagocytosed by each RAW 264.7 cell (Fig. 2 A,B *FITC MFI*). Therefore, DFP enhanced the efficiency of phagocytosis by RAW 264.7 cells. This effect was significant in all the culture conditions ($p = 0.0004$ for Control, $p = 0.0007$ for IL-4, $p = 0.0045$ for LPS) but most prominent in the LPS-treated group. This

data is consistent with the finding that DFP decreased the production of IL-10 induced by LPS. This decrease in IL-10 may play a contributing role to the increased efficacy of phagocytosis of LPS-polarized RAW 264.7 cells.

Once macrophages phagocytose their targets, they can kill by several mechanisms. The most characterized mechanism is the release of reactive oxygen species (ROS) which includes both hydrogen peroxide (H_2O_2) and nitric oxide (NO). We tested the ability of RAW 264.7 cells, polarized with IL-4 and LPS, to make ROS. H_2O_2 and NO can be detected fluorometrically using fluorescent substrates (Amplex Red for H_2O_2 and DAF2-DA for NO). RAW 264.7 cells, even when polarized to M1 macrophages do not make detectable amounts of H_2O_2 (Fig. 2C). Unpolarized or IL-4 polarized RAW 264.7 cells make detectable amounts of NO, however, LPS polarized macrophages make significantly more NO ($p = 0.0003$) (Fig. 2D). Thus, RAW 264.7 cells can make NO at a resting state, but this is significantly increased when they are polarized to M1 macrophages. Unlike what we observed in the phagocytosis and cytokine experiments, the addition of DFP does not seem to enhance their ability to make NO.

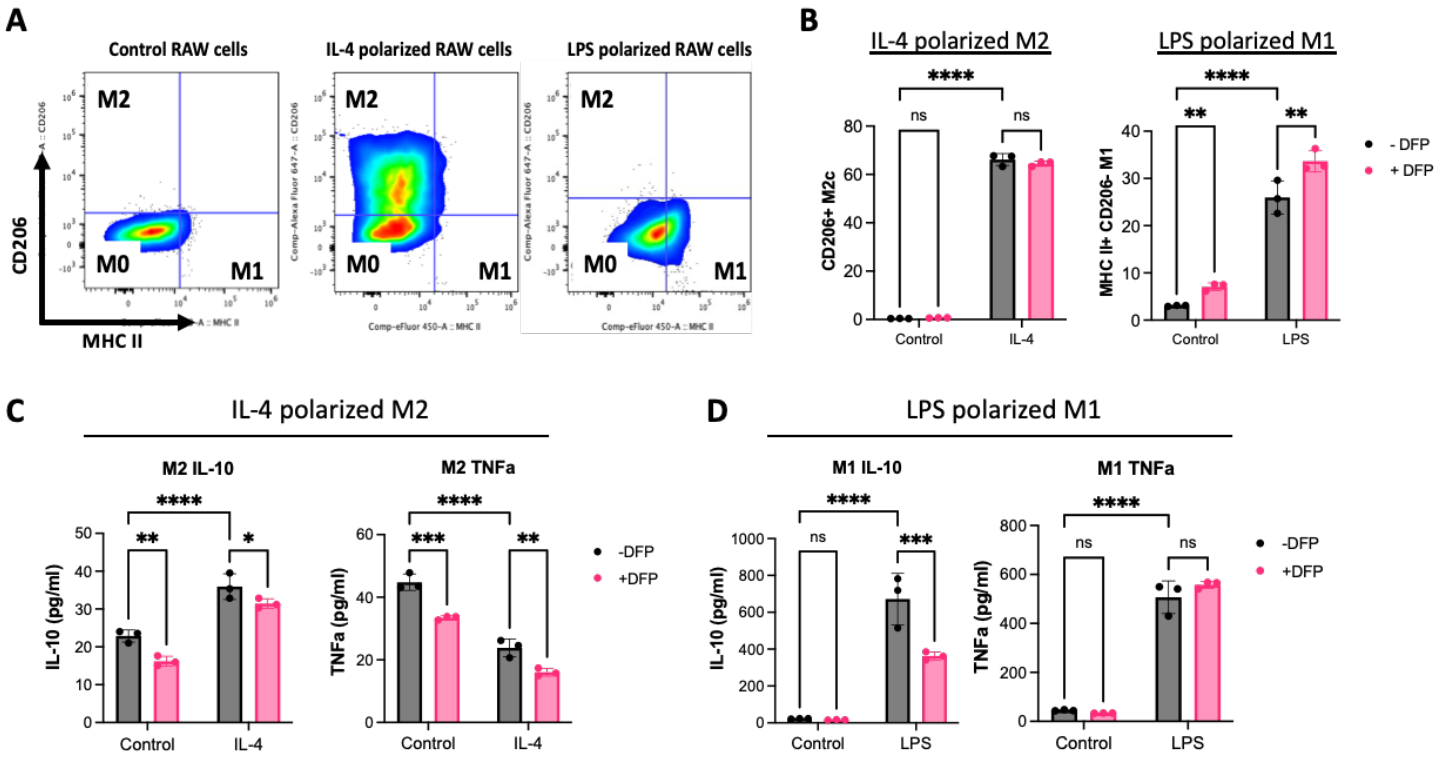

Figure 1: The effects of DFP on macrophage polarization and cytokine production. RAW 264.7 cells were seeded in 24-well plates, treated with IL-4, LPS and/or DFP and incubated for 48 hrs. **A, B**. For phenotypic studies, cells were detached and stained for fluorophore conjugated CD206 and MHC II antibodies for flow cytometry. Shown are representative bivariate plots of MHC II versus CD206 expression (**A**) and quantification of M2 and M1 macrophage polarization (**B**) (n = 1). **C, D.** Cell culture supernatants were collected and analyzed for cytokines using the Luminex multiplex assay. Shown are the amounts of IL-10 and TNFα produced by RAW 264.7 cells polarized to M2 (**C**) or M1 phenotypes (**D**) from triplicates samples from one representative experiment (n = 2 experiments performed). Statistics were calculated using 2-way ANOVA (*p<0.05, **p<0.01, ***p<0.001, ****p<0.0001).

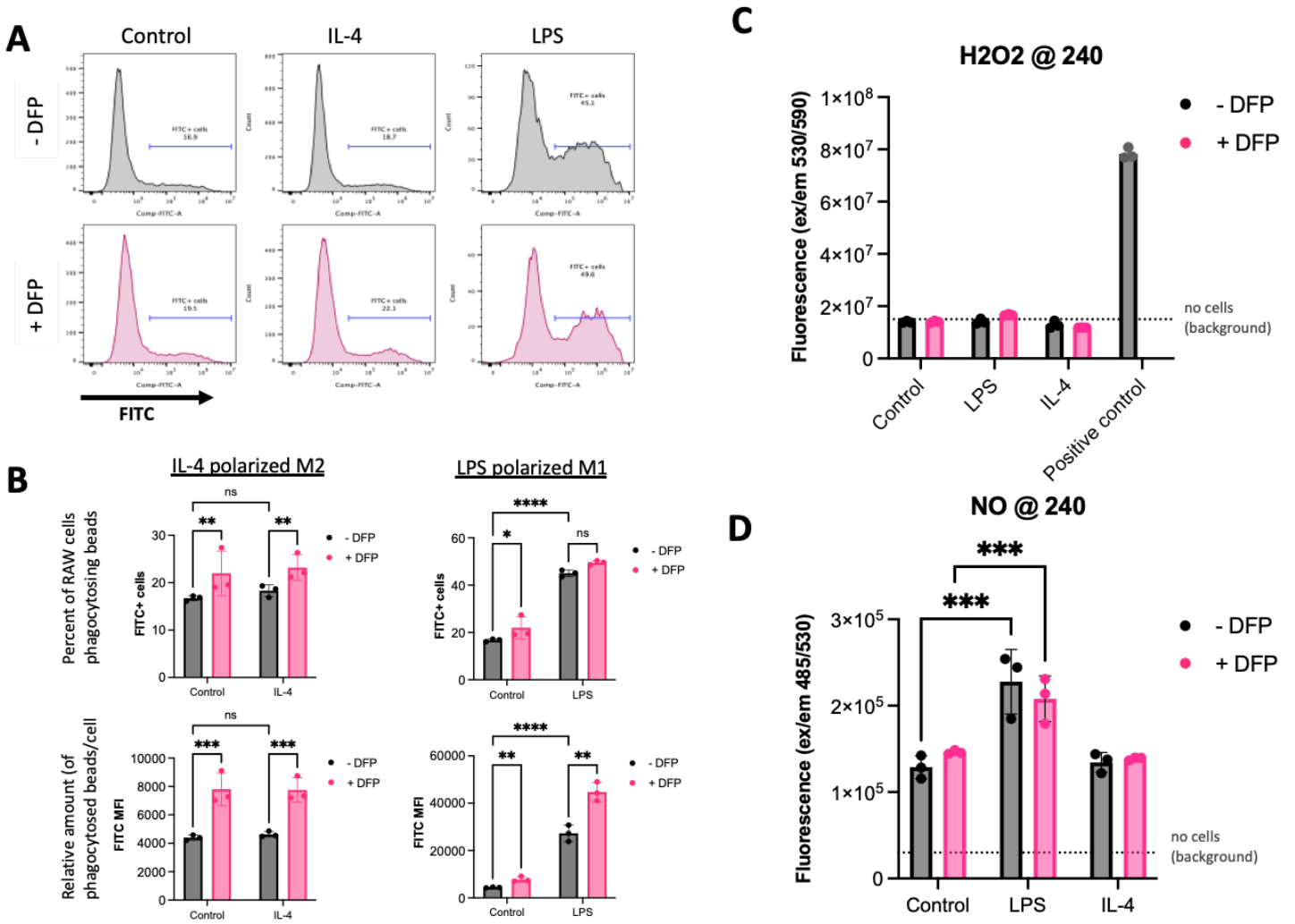

Figure 2: The effects of DFP on macrophage phagocytosis and ROS production. RAW 264.7 cells were seeded in 24-well plates, treated with IL-4, LPS and DFP and incubated for 48 hrs. **A, B.** For phagocytosis: PBS-containing FITC-beads were added to each well and incubated at 37 ºC for 2 hrs. Cells were detached and resuspended in 50 µl Trypan Blue to quench non-phagocytosed beads, stained with a viability dye and then analyzed by flow cytometry. **A** Representative histogram plots of RAW264.7 cells that have taken up FITC beads. **B** Quantification of phagocytosing cells (FITC+ cells, top) and the mean fluorescence (MFI, bottom) of the beads that have been phagocytosed (n = 1). **C, D** For ROS production: 50,000 polarized RAW 264.7 cells were plated in 96-well flat bottom plates in the presence of Amplex Red substrate solution (H_2O_2) or DAF2-DA substrate solution (NO). Fluorescence was determined at an excitation/emission of 530/590 for H_2O_2 and 485/530 for NO every 30-60 mins for up to 240 mins. For the positive control condition, diluted H_2O_2 was added into a control well at 240 mins. Shown are relative fluorescence (n = 1). Statistics were calculated using 2-way ANOVA (*p<0.05, **p<0.01, ***p<0.001, ****p<0.0001).

References

1. Ernst O, Glucksam-Galnoy Y, Bhatta B, Athamna M Ben-Dror I, Glick Y, Gerber D, Zor T. Exclusive Temporal Stimulation of IL-10 Expression in LPS-Stimulated Mouse Macrophages by cAMP Inducers and Type I Interferons Front Immunol 2019 Aug 6;10:1788

2. Pengal RA, Ganesan LP, Wei G, Fang H, Ostrowski MC, Tridandapani S. Lipopolysaccharide-induced production of interleukin-10 is promoted by the serine/threonine kinase Akt. Mol Immunol . 2006 Apr;43(10):1557-64.

Section 2: Tumor Cell Doubling Time in Response to DFP (Koutcher Laboratory) (Aim 1B)
In addition to the proposed cell lines under study, we also investigated the effect of DFP on BT-474 cells, after discussion with Dr. Shuman-Moss. We did this after we advised her that our preliminary in vivo studies with Deferiprone in 4T1 and MDA-MB-231 tumors were disappointing. She agreed that it was reasonable to try the study on an additional different tumor model. We chose the BT-474 HER2$^+$ breast cancer model purposely because it is not a triple negative breast cancer (TNBC) model (both, MDA-MB-231 and 4T1 are TNBC). It is a model for clinical HER2-positive breast cancer, a very common and difficult to treat tumor. Our initial in vitro studies are presented below. These include measurements of tumor cell doubling time, EC50 (50% inhibitory or effective concentration), and EC90 (concentration of DFP affecting 50% and 90% of cells respectively). We include these data with our studies of the 4T1 and MDA-MB-231 doubling time measurements as proposed. We report 1) doubling times for the 3 tumor cell lines and 2) EC50, EC90 of the BT474 to deferiprone. The EC50 and EC90 data for 4T1 and MDA-MB-231 were presented previously.

Methods
For EC50 experiments, 1x10^5 BT-474 cells (ATCC) were seeded per well in 3 separate 12 well plates for each experiment (Falcon® 12-well Clear Flat Bottom TC-treated Multiwell Cell Culture Plate, with Lid, Individually Wrapped, Sterile, 50/Case, Product Number 353043) and allowed to attach for 24 h. For the cell doubling time experiments, 3.2x10^4 and 1.3x10^5 for untreated and DFP-treated 4T1 cells (Fred R. Miller, Karmanos Cancer Institute, Detroit, Michigan) respectively, 5x10^4 MDA-MB-231 cells (ATCC), 6x10^4 BT-474 cells (ATCC), and 9x10^4 RAW 264.7 cells (ATCC) were seeded per well in 24-well plates (Corning 3524 or BD Falcon 353047) and allowed to attach for 24 h. Cell culture media was prepared by the Media Preparation Facility (Dulbecco's Modified Essential Medium containing 25 mM Glucose (Thermo Fisher Scientific, Cat # 12100), supplemented with 2 mM glutamine to a final concentration of 6 mM Glutamine and supplemented with 10% Fetal bovine serum, 100 U/ml Penicillin and 100 µg/ml Streptomycin). Deferiprone was purchased from Toronto Research Chemicals (Cat#D4740000) and stored as a solid at -20 ^{o}C and, for the duration of the experiment, in solution at 4 ^{o}C.

For EC50 experiments after 24 h, the cell culture medium was exchanged for culture medium with 0 µM, 16 µM, 30 µM, 66 µM, 100 µM, 160 µM, 300 µM, 660 µM, 1000 µM for every 3 wells, respectively. Then cells were grown for an additional 72 h with daily medium change. At ~73 h, cells were harvested by trypsinization and counted with a Luna cell counter using the Trypan Blue exclusion assay. For each experiment, the total number of live cells for each sample were averaged over the triplicate samples and the corresponding effective concentration to achieve 50% and 90% effect respectively calculated as described below:

$$100 \cdot \frac{T - T0}{C - T0}, \text{ with}$$

T0: Number of viable cells at time 0 (~24 h post seeding and pre-treatment)
C: Number of viable cells in untreated control cells at time t
T: Number of viable cells at time t

Fitting equation for EC50 (50% effect between top and bottom plateau, with top plateau 100 % (untreated control)), using a 4-parameter fit, i.e. fitting of Top, Bottom, HillSlope and LogEC50:

$$Y = Bottom + \frac{Top - Bottom}{1 + 10^{(LogEC50 - LogDrugDose) \cdot HillSlope}}$$

Calculation of $EC_{anything}$ (e.g. used to calculate EC90):

$$logEC50 = logECF - (1/HillSlope) * log(F/(100-F)), \text{ with}$$

F: Constant between 0 and 100, referring to the percentage between top and bottom plateau (e.g. 50 for ED50, 10 for EC90, as the Y response decreases with increasing drug dose).

For cell doubling time experiments after 24 h, 3 triplicated wells were counted for each cell line (and for 4T1 for both seeding densities) to obtain a time zero count. Then, the cell culture medium was exchanged for culture medium with 0 µM or 100 µM DFP for 24 wells (1 plate for each cell type & condition), respectively. Every 24 h, the medium was exchanged for fresh culture medium with or without DFP to avoid nutrient depletion and medium acidification. At the same time, cells in 3 wells for each cell type & condition were harvested every 24

h until at least ~ 2 cell doubling times had past and counted with the Trypan Blue exclusion assay using a Luna cell counter (Logos Biosystems, Annandale, VA). The natural logarithm of the cell number at each time point was plotted over the growth time and fitted by linear regression to obtain the cell doubling time. The resulting cell doubling times were averaged for each cell line and condition and the standard error calculated. As the growth rate is inhibited by DFP, we performed a one-tailed T test to compare the doubling times of DFP-treated with untreated cells. Where each independent experiment that had both, treated and untreated cells (here for BT-474), the T Test was paired, while otherwise an unpaired T test was performed (all other cell lines and conditions).

Results

Fig. 1A shows a typical EC50 experiment curve. In this model, deferiprone is largely cytostatic but does also include some cytotoxicity effects. The EC50 was measured as 43.5 ± 6.2 µM which is comparable to that found previously for the other breast and prostate cancer cell lines and provided in the 2018 report.

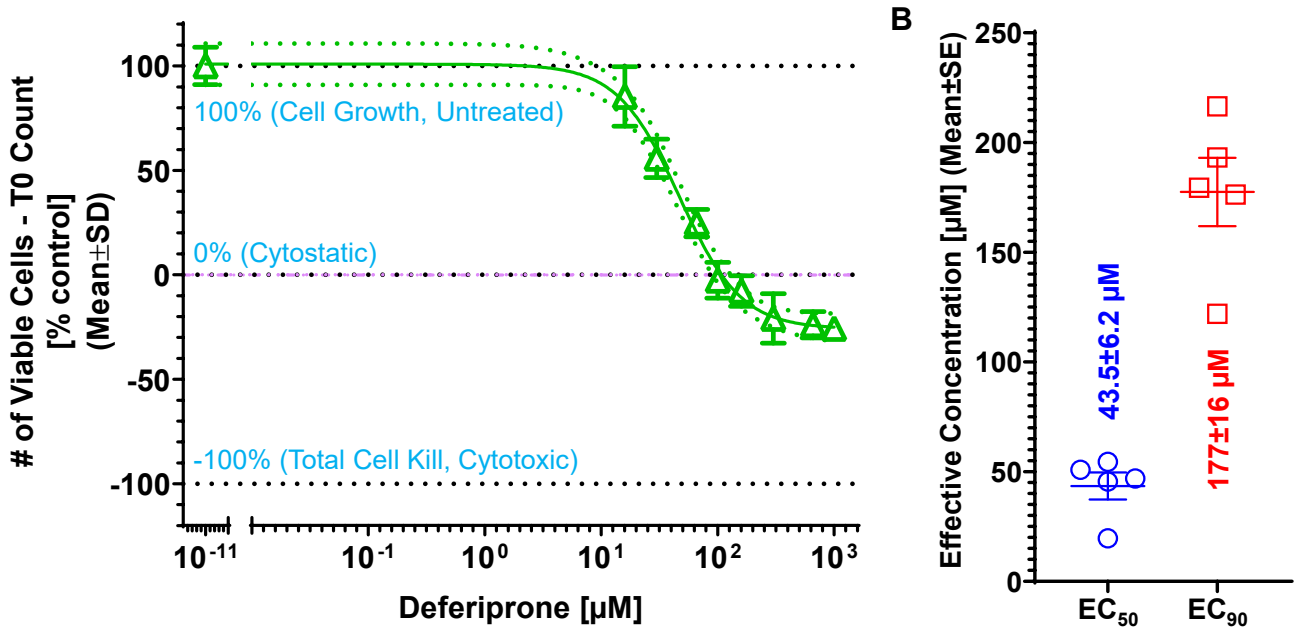

Figure 1: Effect of Deferiprone on BT-474 cells. (**A**) A representative curve displaying the effect of a 73 hours exposure of BT-474 cells to increasing DFP concentrations on the cell growth and viability. T0 count is the number of viable BT-474 cells at the start of the exposure. (**B**) Average EC50 and EC90 values for BT-474 cells from 5 independent experiments with triplicate samples within each experiment.

Figure 2A show the natural logarithm of the cell numbers at various time points and the corresponding linear fits with 95% confidence intervals of the fits used to calculate the doubling times for each independent experiment. For each separate independent experiment, each time point is the average of 3 replicates. Figure 2B summarized the cell doubling times for 4 cell lines, untreated or exposed to 100 µM DFP. Deferiprone significantly reduces the growth rate, i.e. prolongs the cell doubling times, in 4T1 and BT-474 cells. The same effect is observed for MDA-MB-231 cells, though there are currently only 2 (1 additional study ongoing, hence 1 time point missing) experiment for untreated MDA-MB-231 cells. We are in the process of adding 2 additional experiments. We will also complete the doubling time experiments for RAW 264.7 cells and will present the results in the final report.

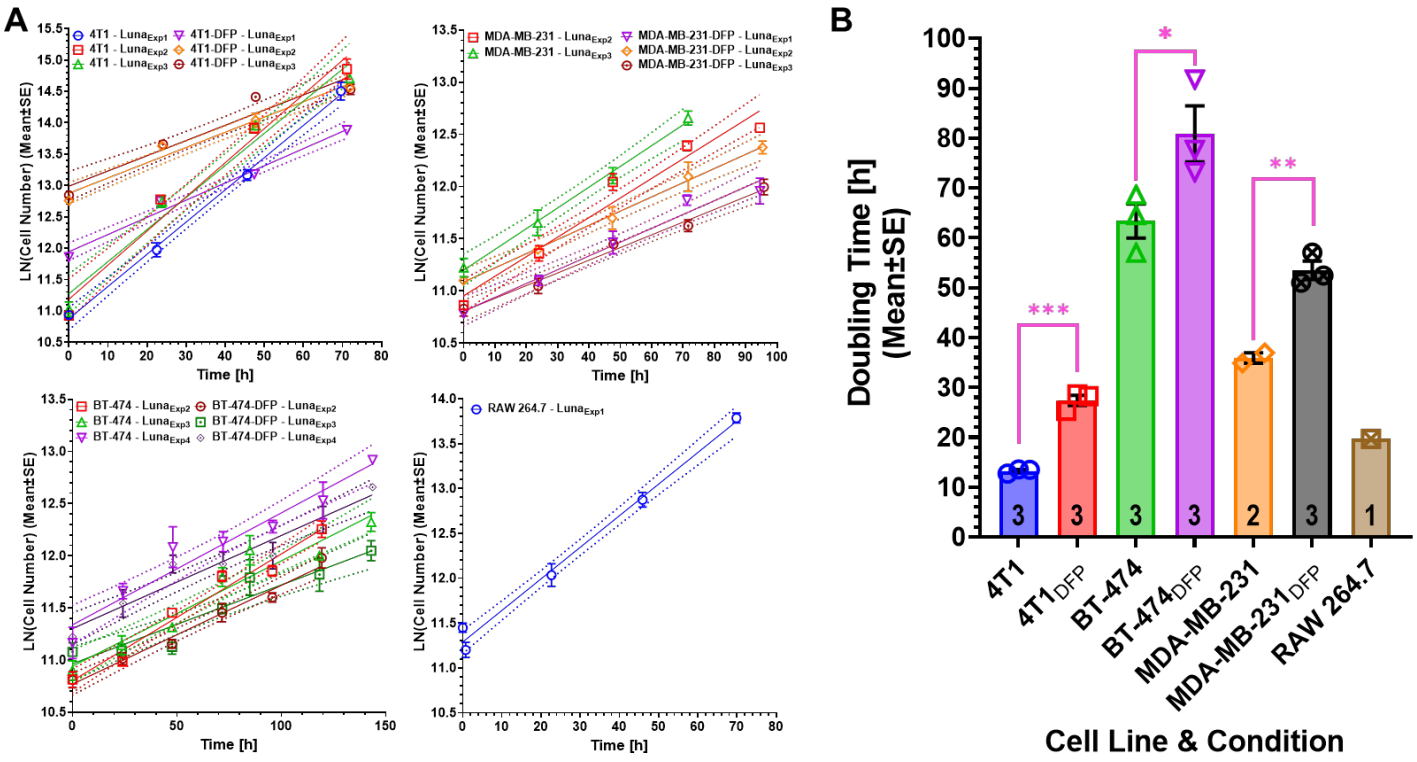

Figure 2. Effect of DFP on in vitro cell growth. (**A**) Natural logarithm of the cell numbers obtained from triplicate samples at each time point and the corresponding linear fits with 95% confidence intervals of the fits for each independent experiment for 4T1 (top left), MDA-MB-231 (top right), BT-474 (bottom left), and untreated RAW 264.7 cells. (**B**) Average cell doubling times for untreated and DFP-treated cells. Deferiprone significantly reduces cell growth in BT-474 ($p = 0.0139$, 1-tailed, paired T test), 4T1 cells ($p = 0.0009$, 1-tailed, unpaired T-test assuming both populations have the same standard deviation) and MDA-MB-231 cells ($p = 0.0029$, 1-tailed, unpaired T-test assuming both populations have the same standard deviation). * $p<0.05$, ** $p<0.01$; *** $p<0.001$.

Section 3: Cell Migration Studies (Koutcher Laboratory) (Aim 1)

Studies on 4T1 were presented in 2019. Data below are for MDA-MB-231.

TNBC Cell Migration - Methods

The effect of deferiprone (DFP) exposure on the migration of 4T1 and MDA-MB-231 cells was assessed in up to 6 independent experiments per time point per cell line using the wound healing assay.[1] For each experiment, a 24-well plate (Falcon® Plates, Corning Life Sciences, Teterboro, NJ, USA) was seeded per well with 3.1×10^4 4T1 cells or 25×10^4 MDA-MB-231 cells in 0.4 ml culture medium. Cells were cultured until reaching a confluent monolayer in each well, which was scraped with a plus sign motion (Fig. 1A) 48 hours and 3-3.5 days after the seeding of 4T1 and MDA-MB-231 respectively using a standard 200 µl pipette tip.[1-3] Wells were subsequently washed once with phosphate-buffered saline (PBS) to remove the cellular debris, and each of them refilled with 0.4 ml of medium containing either no DFP (control = 0 µM DFP), 50 µM DFP, or 100 µM DFP corresponding to three different treatment conditions. The culture medium was changed every 24 h post seeding to avoid nutrient depletion and medium acidification. Following a pilot experiment to assess the timing of the wound closures for each cell line, the total imaging time to monitor cell migration into the cell-free area was set to 48 hours for 4T1 and 60-72 hours for MDA-MB-231 cells, with 12 hour time resolution for both of them. For each cell line, one image per plate was acquired approximately 1 hour after DFP exposure (t = 0) and then every 12 hours through brightfield microscopy (ZEN microscope, Carl Zeiss, Germany) using a 5× objective lens and 45 frames per well. Using the ZEN software, a single image of each well was obtained at each time point by stitching the frames together and exporting to Tiff format for further processing, which includes the image conversion to 8-bit, the background subtraction with the subsequent application of filters such as de-speckling and unsharp filters followed by the variance and Gaussian blur filters. To automate the image processing and determine the open wound area per well at each time point, a custom-written macro in Fiji (ImageJ; https://imagej.nih.gov/ij/)[4] was used. For each cell line, a mean relative open wound area was calculated for each treatment condition and time point per experiment by dividing the absolute open wound area in μm^2 for each well by the average of the absolute open wound area in μm^2 in all wells at t = 0, as described before.[2, 3] This allowed the investigators to account for the inter- and intra-experimental variations at the start of each experiment. For each independent experiments and cell line, the mean and standard deviation (SD) of the relative open wound area were calculated for each condition and time point. Then for each cell line, the mean average relative open wound area at each time point and for each condition was averaged for the up-to 6 independent experiments and the corresponding SD calculated by error propagation (maximum error, assuming Gaussian distribution). For the latest time points, when all wells per experiment and treatment condition had a fully closed wound area (relative open wound area = 0%, see e.g. Fig. 1A at ~48 h for 50 µM and 100 µM DFP), the measurement error was defined to be zero.

Results

Figure 1A shows the effects of the “scratch” on tumor growth using 0 µM (control), 50 µM and 100 µM DFP. Figure 1B shows that cells treated with DFP had a modestly greater cell migration at 24 hours, which is different than what was noted with the 4T1 cells. As presented in the 2019 report, exposure of 4T1 cells to 100 µM DFP (~EC90 for 4T1 cells) delays full wound closure (i.e. inhibits cell migration required in the metastatic process) to 48 h, resulting in a significantly higher relative open wound area at 24 h ($P<0.0001$) and 36 h ($P=0.0003$) compared to untreated 4T1 cells and 4T1 cells treated with 50 µM DFP. In both cell lines, wound closure is dominated by migration within the first doubling time and after that influenced by both, cell migration and growth. Thus, wound closure differences in response to DFP between 4T1 and MDA-MB-231 may be due to their different growth rates depicted in Section 2, Figure 2 (cell doubling time).

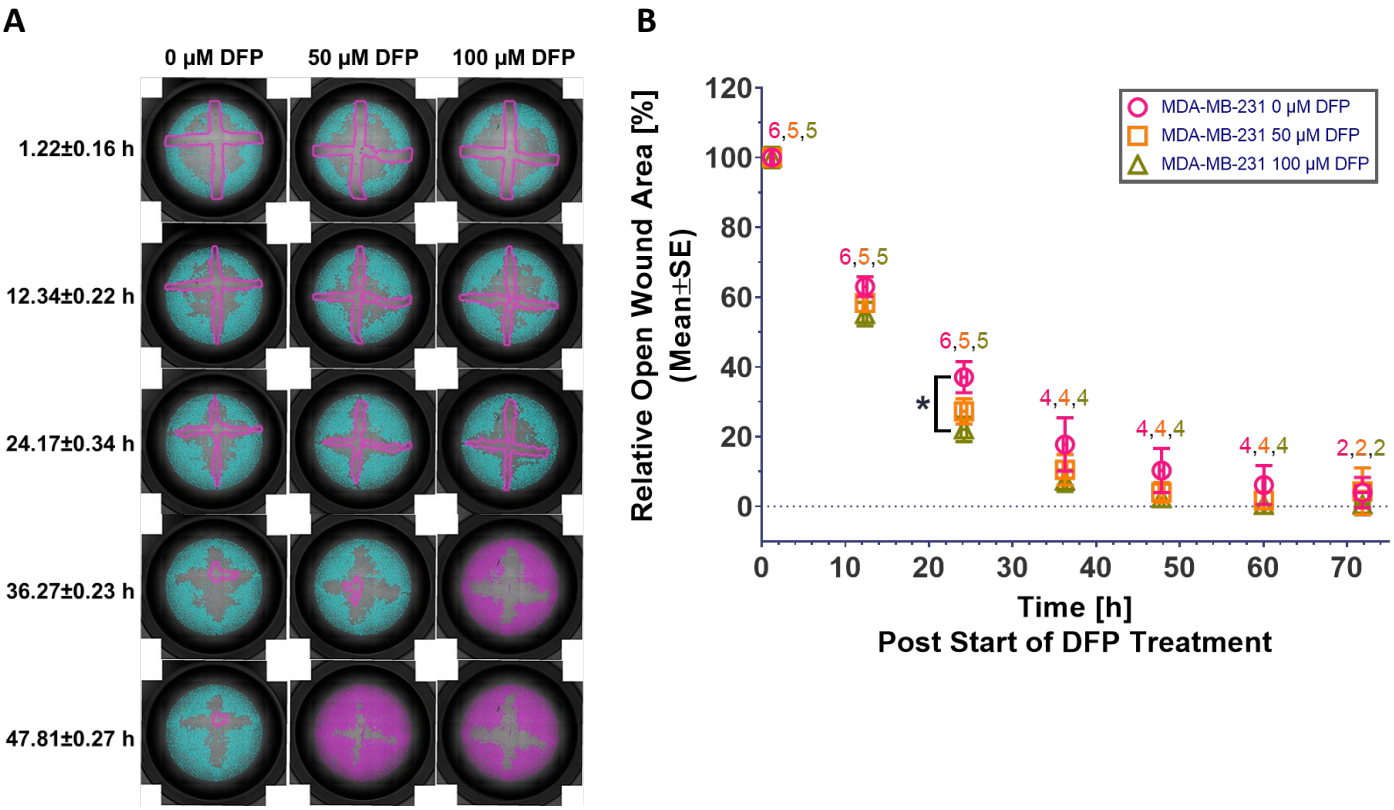

Figure 1: Wound healing assay for MDA-MB-231 cells exposed to DFP for up-to 72 h. **(A)** Single sample well images overlaid with outlines of open wound area (cross in center outlined in pink) at different time points; cyan indicates thresholded cell counts outside of scratch, while darker pink (at 36 and 48 hours) indicates threshold for cell counts when the wound has been closed with cells and no open wound area can be detected. , No open wound area is left in the 100 µM DFP ~36 h and ~48 h and in the 50 µM DFP samples at ~48 h. Due to differences in contrast between dense cells outside of the original wound area and the single layer, flatter cells migrated into the wound area, a single threshold is not a reliable way to assess cell counts and leads to the cell count void visible in the images when the wound area is closed. (Hence, cell counts have not been used, due to described difficulty of reliable cell counts in dense samples across the wells using these images). **(B)** Wound closures in untreated and treated MDA-MB-231 cells averaged over 2-6 independent experiments (indicated for each condition color-coded above each average), with 3-6 repeats within each experiment. As can be seen from the somewhat faster wound closure, cell migration increased in cells exposed to increasing doses of deferiprone, reaching significance between control and 100 µM DFP only at 24.17±0.34 h ($p<0.05$). At later time points, control cells catch up with the wound closure which might in part be explained by their faster cell doubling time DT than the DT for cells exposed to DFP (see Fig. 2 in section 2 (above – cell doubling times)).

References:

1. Liang CC, Park AY, Guan JL. In vitro scratch assay: a convenient and inexpensive method for analysis of cell migration in vitro. Nat Protoc. 2007;2(2):329-33. Epub 2007/04/05. doi: 10.1038/nprot.2007.30. PubMed PMID: 17406593.

2. Geback T, Schulz MM, Koumoutsakos P, Detmar M. TScratch: a novel and simple software tool for automated analysis of monolayer wound healing assays. Biotechniques. 2009;46(4):265-74. doi: 10.2144/000113083. PubMed PMID: 19450233.

3. Simoes RV, Veeraperumal S, Serganova IS, Kruchevsky N, Varshavsky J, Blasberg RG, Ackerstaff E, Koutcher JA. Inhibition of prostate cancer proliferation by Deferiprone. NMR Biomed. 2017;30(6). Epub 2017/03/09. doi: 10.1002/nbm.3712. PubMed PMID: 28272795 PubMed Central PMCID: PMC5505495.

4. Schindelin J, Arganda-Carreras I, Frise E, Kaynig V, Longair M, Pietzsch T, Preibisch S, Rueden C, Saalfeld S, Schmid B, Tinevez JY, White DJ, Hartenstein V, Eliceiri K, Tomancak P, Cardona A. Fiji: an open-source platform for biological-image analysis. Nature Methods. 2012;9(7):676-82. doi: 10.1038/Nmeth.2019. PubMed PMID: WOS:000305942200021.

Section 4: Testing Corning Dissolvable Microcarriers for feasibility of culturing RAW 264.7 Cells for metabolic studies (Aim 1) (Koutcher Laboratory)

In last year's report, we noted successful completion of metabolic measurements of both MDA-MB-231 and 4T1 cells. We also noted that we had begun parallel measurements on RAW264.7 macrophage cells but had hit a serious impediment in that the cells adhered poorly to the beads which were necessary to keep them alive and stable in the perfusion apparatus. We reported testing different types of microcarrier beads unsuccessfully. We report here that further attempts on some novel commercial beads that were in the "pre-commercial" state were successful. Dissolvable microcarriers (Product Number 7285, Corning®, New York, NY, USA) were tested to culture the RAW 264.7 cells with the aim to monitor cellular and energy metabolism through ^{31}P and ^{13}C magnetic resonance spectroscopy (MRS) while live cells growing on microcarriers in our compatible MR perfusion system.

Dissolvable microcarriers represent a new product from Corning. For this reason, it required a long time for procuring and testing them. They are made of polygalacturonic acid (PGA) polymer chains, cross-linked via calcium ions. When fully hydrated, they have an average size of 200 to 300 µm, suitable for our perfusion system, and a density of 1.01 to 1.03 g / cm^3. We tested them along with the Collagen-coated Microcarriers (Corning, Product Number 3786) after a meeting with the Corning Scientific support team, which allowed us to have different options following the unsatisfactory results obtained by culturing the RAW 264.7 cells on the Enhanced Attachment Microcarrier (Product Number 3779, Corning®, New York, NY, USA), those previously used to culture TNBC cell lines 4T1 and MDA-MB-231.

Hydration of dry dissolvable microcarriers and cell seeding

1 g of dry dissolvable microcarriers were hydrated in 150 ml of sterile water within a siliconized glass bottle of 250 ml (Corning, Cat. No. 1395-250). After gently swirling the suspension, the microcarriers were hydrated for 10 min. To confirm complete hydration, a sample of 2 ml of microcarriers was inspected under the microscope and imaged to compare their hydration state with that recommended in the instructions, as shown in **Fig. 1.**

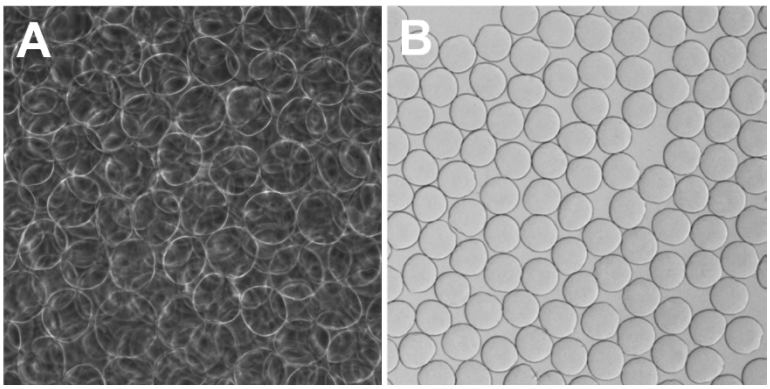

Figure 1. Comparison between fully hydrated dissolvable microcarriers imaged under the microscope (10x magnification) after 10 min hydration time (**A**) and those shown in figure (**B**), provided in the product instructions to confirm the complete hydration by direct comparison.

Subsequently, the water used for microcarrier hydration was exchanged with high glucose DME culture medium added with 2 mM glutamine, the same culture medium used for all other studies in this report, and the microcarriers allowed to settle for 30 minutes. For the seeding procedure, 3×10^6 RAW 264.7 cells were seeded on 0.5 ml of dissolvable microcarriers in:

i. a deep-form bacteriological Petri dish of 25 mm height (n = 3; 100 mm diameter; Cat # 4031, Thermo Scientific Nunc™, Waltham, MA, USA);
ii. an ultra-low attachment bacteriological Petri dish of 20 mm height (n = 1; 100 mm diameter; 20 mm height; Cat # 3262; Corning®, New York, NY, USA);
iii. an ultra-low attachment bacteriological Petri dish of 15 mm height (n = 2; 100 mm diameter; 15 mm height; Cat # 351029; Corning®, New York, NY, USA),

where 15 ml of complete high glucose DME culture medium were added afterwards. The different plates (i), (ii) and (iii) were used to evaluate the best option to adapt for preculturing and growing the cells on microcarriers before loading them into the bioreactor for the cell perfusion experiments.
Immediately after seeding the cells, each plate was inspected under the microscope and imaged at 10x and 20x magnification as shown in **Fig. 2** for a representative plate.

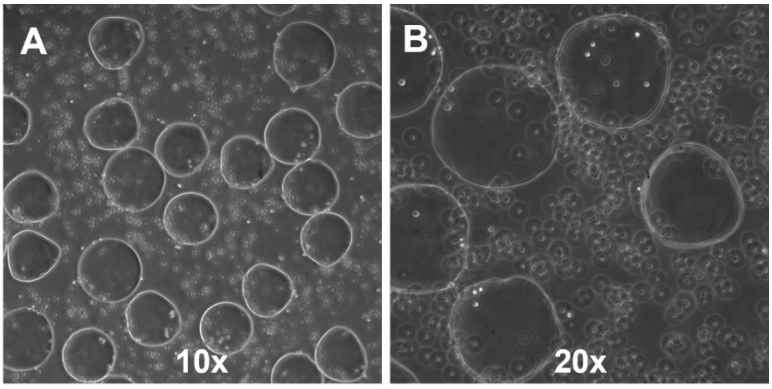

Figure 2. Representative images of dissolvable microcarriers inspected under the microscope and imaged at 10x (**A**) and 20x (**B**) magnification immediately after seeding the RAW 264.7 cells.

Monitoring RAW 264.7 cell growth on dissolvable microcarriers
The RAW 264.7 cells were observed growing on the dissolvable microcarriers for up to four days after the seeding in both, ultra-low-attachment bacteriological Petri dishes of 15 mm height (iii) and one of the deep-form bacteriological Petri dishes of 25 mm height (i); for up to 5 days for the remaining two deep-form bacteriological Petri dishes of 25 mm height (i), indicated as NUNC in some figures, and the ultra-low attachment bacteriological Petri dish of 20 mm height (ii).

Twenty-four hours after cell seeding on the dissolvable microcarriers, the medium was changed in all plates except in one of the two ultra-low attachment bacteriological Petri dishes of 15 mm height (type iii; Plate 1). This exception was made to evaluate whether changing, or not changing the culture medium 24 hours post seeding (on day 1), were both viable options. There was concern that since the dissolvable microcarriers were barely visible, there was a risk of losing them during the medium changing procedure on the first day, hence a possible advantage to not changing the media 24 hours after plating. To evaluate this, images from both Petri dishes, (iii, Plate 1 (**top panel (**media not changed**)**) and Plate 2 (**bottom panel,** media changed at 24 hours), acquired at day 1 before changing the culture medium in plate 2 (**Fig. 3**), and at day 2 (48 hours following the seeding) after changing the medium (**Fig. 4**) in both plates, were compared at 10x (**A**, **D**), 20x (**B**, **E**) and 40x (**D**, **F**) as shown in both **Fig. 3** and **Fig. 4**. The comparison between the images acquired on both Petri dishes at day 1, before changing the culture medium in Plate 2 (**Fig. 3**), and at day 2, immediately after changing the medium in both plates (**Fig. 4**), do not show substantial differences between the cells cultured on microcarriers in both plates. In addition, no acidification process was revealed as indicated by the color of the culture medium in Plate 1 at day 2. These observations along with the high probability of losing a significant number of microcarriers when changing the medium on day 1 because of their low visibility, suggest that not changing the culture medium 24 hour after the cell seeding might be the best procedure to adopt.

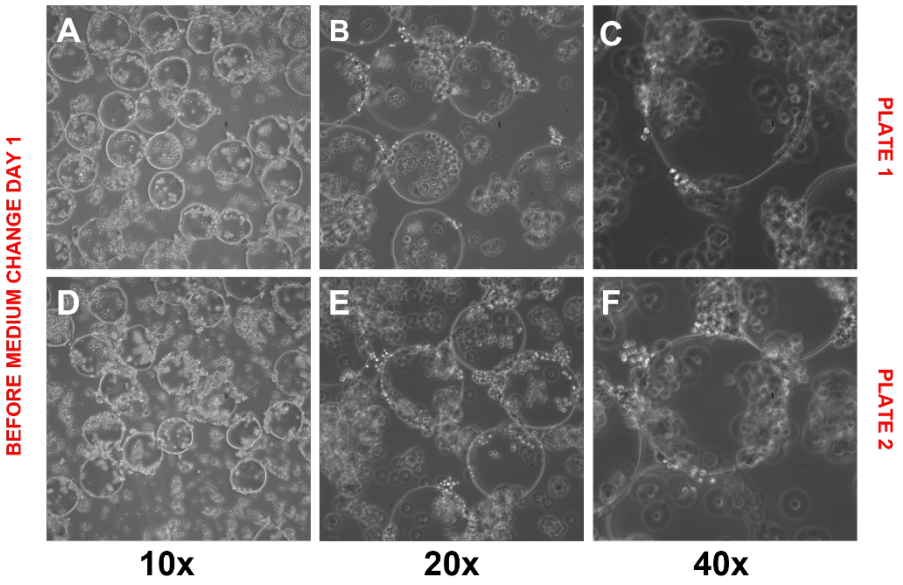

Figure 3. Comparison between images acquired **before** changing the culture medium at day 1 (24 hours following the seeding) from the growing cells on dissolvable microcarriers in the two ultra-low attachment bacteriological Petri dishes of 15 mm height (iii), Plate 1 (**top panel**; **A**, **B**, **C**) and Plate 2 (**bottom panel**; **D**, **E**, **F**). Images **A** and **D**, **B** and **E**, and **C** and **F,** were respectively acquired at 10x, 20x and 40x magnification.

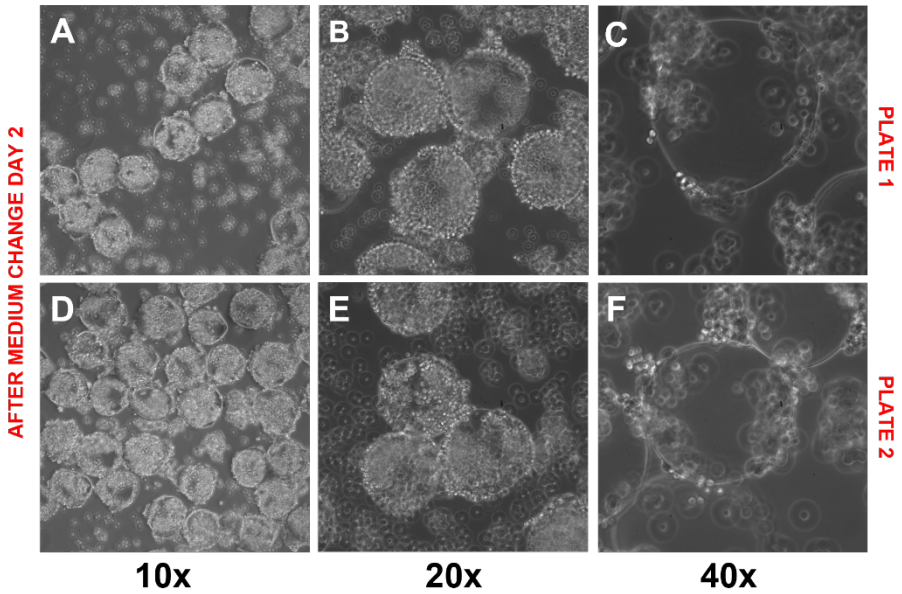

Figure 4. Comparison between images acquired **after** changing the culture medium at day 2 (48 hours following the seeding) from the growing cells on dissolvable microcarriers in two ultra-low attachment bacteriological Petri dishes of 15 mm height (iii), Plate 1 (**top panel**; **A**, **B**, **C**) and Plate 2 (**bottom panel**; **D**, **E**, **F**). Images **A** and **D**, **B** and **E**, and **C** and **F,** were respectively acquired at 10x, 20x and 40x magnification. Qualitatively no differences were noted whether the media was changed at 24 hours or not

After day 1, the culture medium was changed daily in each plate and the growing cells on the dissolvable microcarriers were inspected under the microscope and imaged at 10x, 20x and 40x magnification before and after medium change. Representative images of growing cells on dissolvable microcarriers in different type of plates (i, ii and iii) are shown below for each day following the seeding procedure. **Fig. 5**, **7**, **9** and **12** show the comparison between images of growing cells on dissolvable microcarriers acquired on the same deep-form bacteriological Petri dish of 25 mm height (i) immediately before (**top panel**) and after changing the culture medium (**bottom panel**) at day 1 (24 hour following cell seeding), day 2 (48h), day 3 (72h) and day 4 (96h), respectively. **Fig. 6**, **8**, **10** and **13** show the same type of comparison for the ultra-low attachment bacteriological Petri dish of 20 mm height (ii) at day 1, day 2, day 3 and day 4, respectively. Both ultra-low

attachment bacteriological Petri dishes of 15 mm height (iii), which were used to evaluate whether changing medium 24 hours following the seeding (**Fig. 3** and **4**), were inspected each day and harvested on day 4 (96 hour following cell seeding). Representative images of one of the plates (iii) at day 3 (72h following cell seeding) are shown in **Fig. 11**.

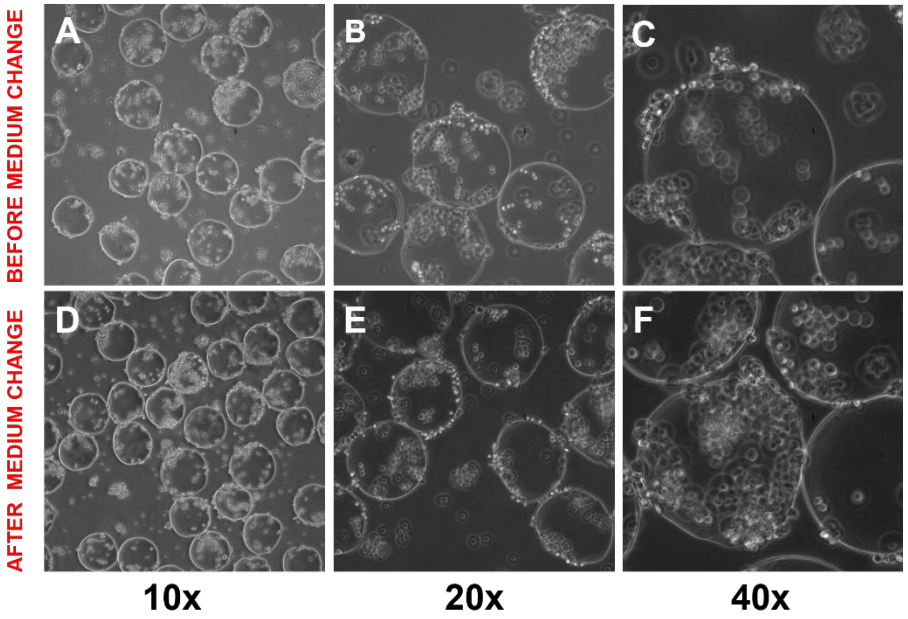

Figure 5. Representative images of growing cells on dissolvable microcarriers in a deep-form bacteriological Petri dish of 25 mm height (i) inspected under the microscope before (**top panel**; **A**, **B**, **C**) and after changing the culture medium (**bottom panel**; **D**, **E**, **F**) at day 1 (24 hours following cell seeding). Images were acquired at 10x (**A**, **D**), 20x (**B**, **D**) and 40x (**C**, **F**) magnification.

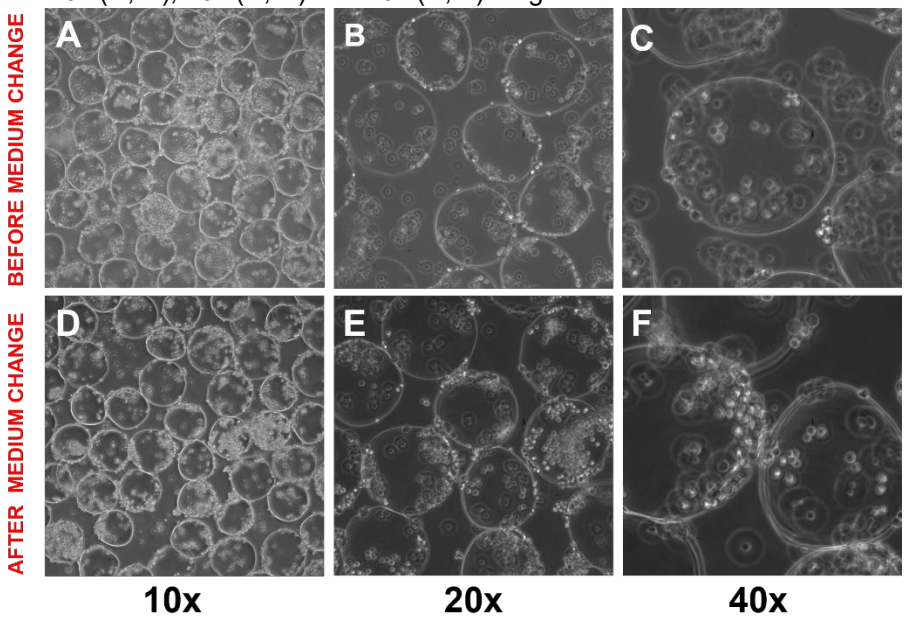

Figure 6. Representative images of growing cells on dissolvable microcarriers in the ultra-low attachment bacteriological Petri dish of 20 mm height (ii) inspected under the microscope before (**top panel**; **A**, **B**, **C**) and after changing the culture medium (**bottom panel**; **D**, **E**, **F**) at day 1 (24 hours following cell seeding). Images were acquired at 10x (**A**, **D**), 20x (**B**, **D**) and 40x (**C**, **F**) magnification.

The comparisons between **Fig. 5** and **6**, **Fig. 7** and **8**, **Fig. 9** and **10**, and **Fig. 12** and **13** respectively acquired at day 1, 2, 3 and 4 on microcarriers growing on a representative deep-form bacteriological Petri dishes (i) (**Fig. 5**, **7**, **9**, **12**) and on those growing on the ultra-low attachment plate (ii) (**Fig. 6**, **8**, **10**, **13**) do not show any difference depending on the type of plate used. The same consideration was revealed by comparing **Fig 9**, **10** and **11** acquired at day 3 respectively on cells growing on microcarriers in a representative deep-form

bacteriological Petri dishes (i) (**Fig. 9**) and on those growing on the ultra-low attachment plate (ii) (**Fig. 10**) and on a representative plate (iii) (**Fig. 11**). The absence of substantial differences between cells growing on microcarriers in the different type of plates (i, ii, iii) suggest the use of the deep-form bacteriological Petri dishes as more appropriate because their height (25 mm) is easier for handling.

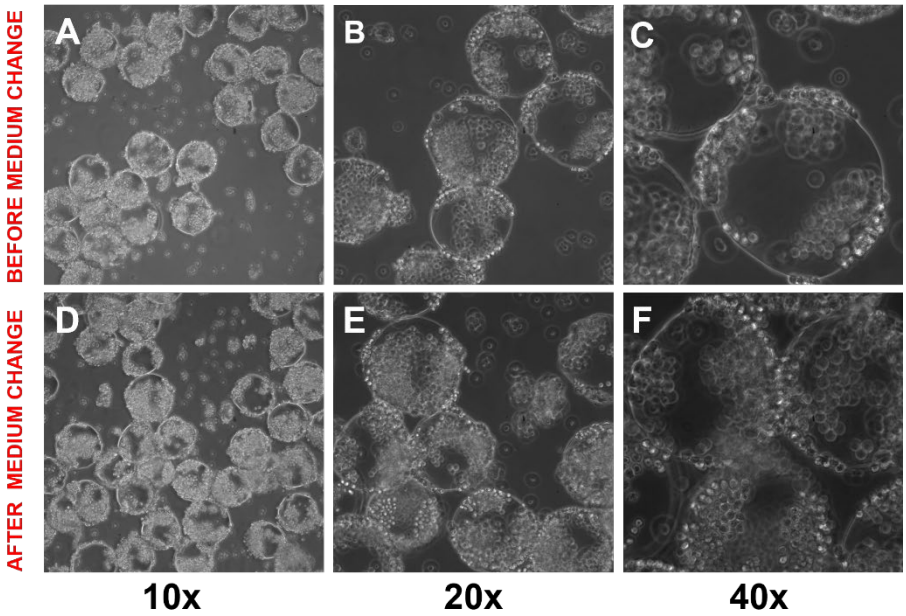

Figure 7. Representative images of growing cells on dissolvable microcarriers in a deep-form bacteriological Petri dish of 25 mm height (i) inspected under the microscope before (**top panel**; **A**, **B**, **C**) and after changing the culture medium (**bottom panel**; **D**, **E**, **F**) at day 2 (48 hours following cell seeding). Images were acquired at 10x (**A**, **D**), 20x (**B**, **D**) and 40x (**C**, **F**) magnification.

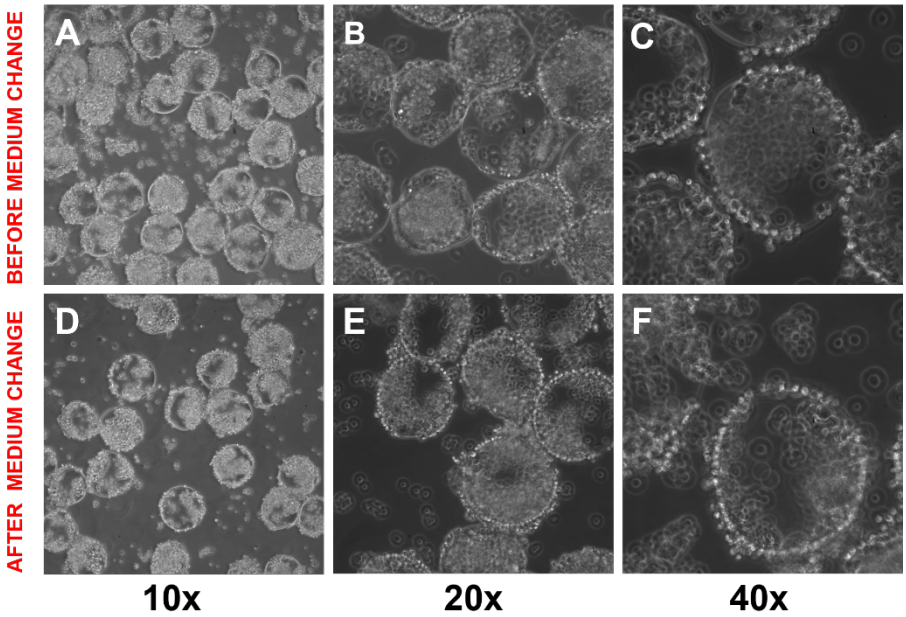

Figure 8. Representative images of growing cells on dissolvable microcarriers in the ultra-low attachment bacteriological Petri dish of 20 mm height (ii) inspected under the microscope before (**top panel**; **A**, **B**, **C**) and after changing the culture medium (**bottom panel**; **D**, **E**, **F**) at day 2 (48 hours following cell seeding). Images were acquired at 10x (**A**, **D**), 20x (**B**, **D**) and 40x (**C**, **F**) magnification.

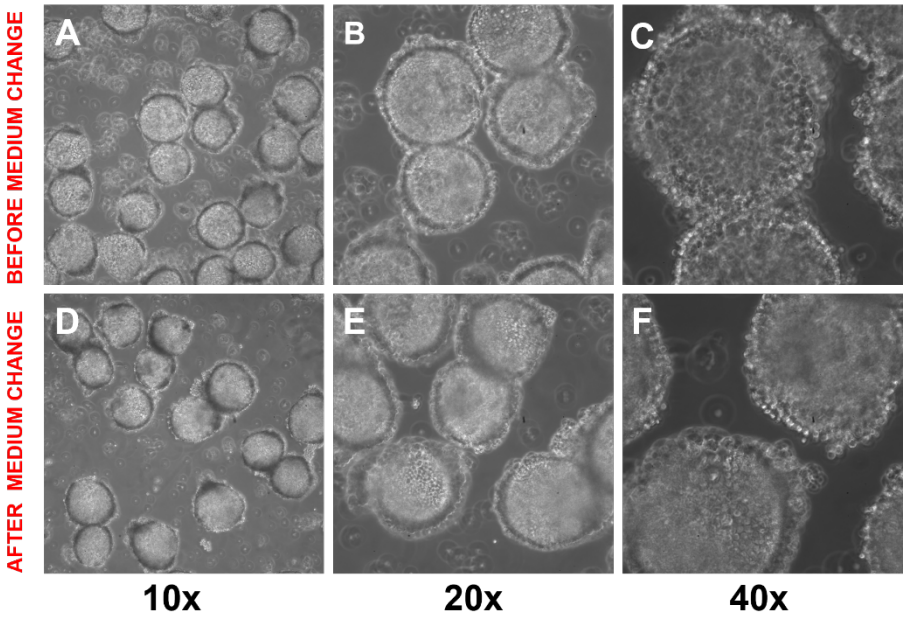

Figure 9. Representative images of growing cells on dissolvable microcarriers in a deep-form bacteriological Petri dish of 25 mm height (i) inspected under the microscope before (top panel; **A**, **B**, **C**) and after changing the culture medium (bottom panel; **D**, **E**, **F**) at day 3 (72 hours following cell seeding). Images were acquired at 10x (**A**, **D**), 20x (**B**, **D**) and 40x (**C**, **F**) magnification.

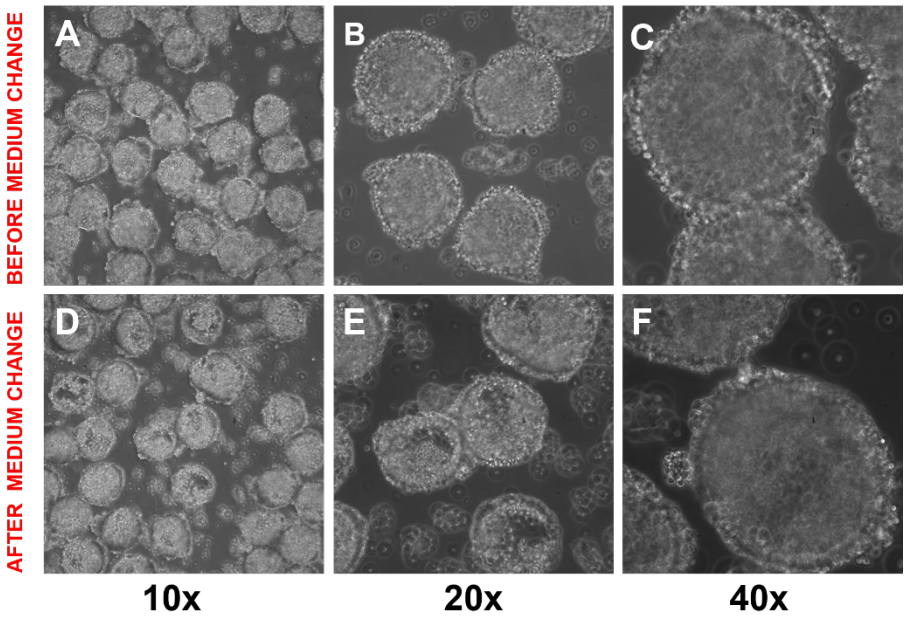

Figure 10. Representative images of growing cells on dissolvable microcarriers in the ultra-low attachment bacteriological Petri dish of 20 mm height (ii) inspected under the microscope before (**top panel**; **A**, **B**, **C**) and after changing the culture medium (**bottom panel**; **D**, **E**, **F**) at day 3 (72 hours following cell seeding). Images were acquired at 10x (**A**, **D**), 20x (**B**, **D**) and 40x (**C**, **F**) magnification.

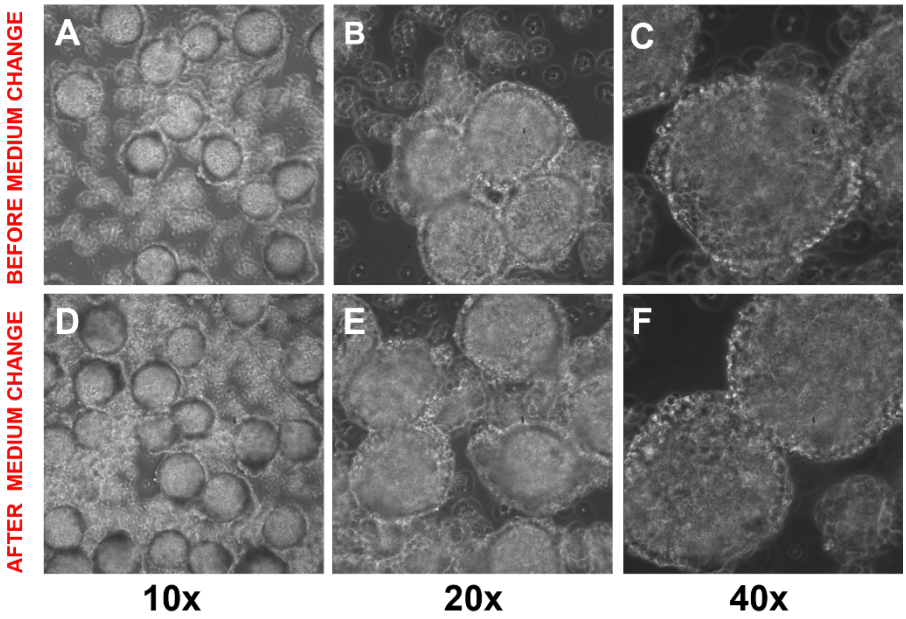

Figure 11. Representative images of growing cells on dissolvable microcarriers in an ultra-low attachment bacteriological Petri dish of 15 mm height (iii) inspected under the microscope before (**top panel**; **A**, **B**, **C**) and after changing the culture medium (**bottom panel**; **D**, **E**, **F**) at day 3 (72 hours following cell seeding). Images were acquired at 10x (**A**, **D**), 20x (**B**, **D**) and 40x (**C**, **F**) magnification.

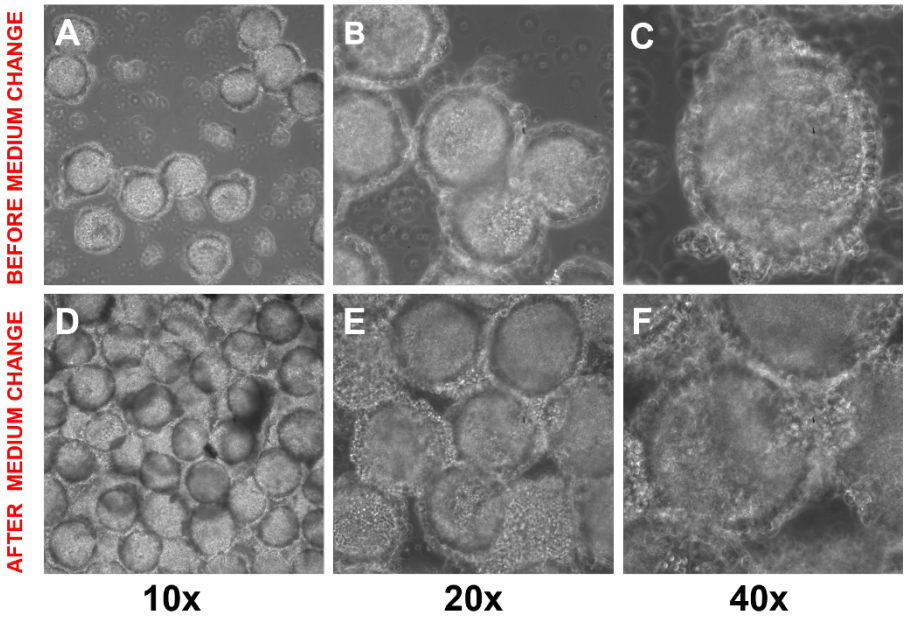

Figure 12. Representative images of growing cells on dissolvable microcarriers in a deep-form bacteriological Petri dish of 25 mm height (i) inspected under the microscope before (top panel; **A**, **B**, **C**) and after changing the culture medium (bottom panel; **D**, **E**, **F**) at day 4 (96 hours following cell seeding). Images were acquired at 10x (**A**, **D**), 20x (**B**, **D**) and 40x (**C**, **F**) magnification.

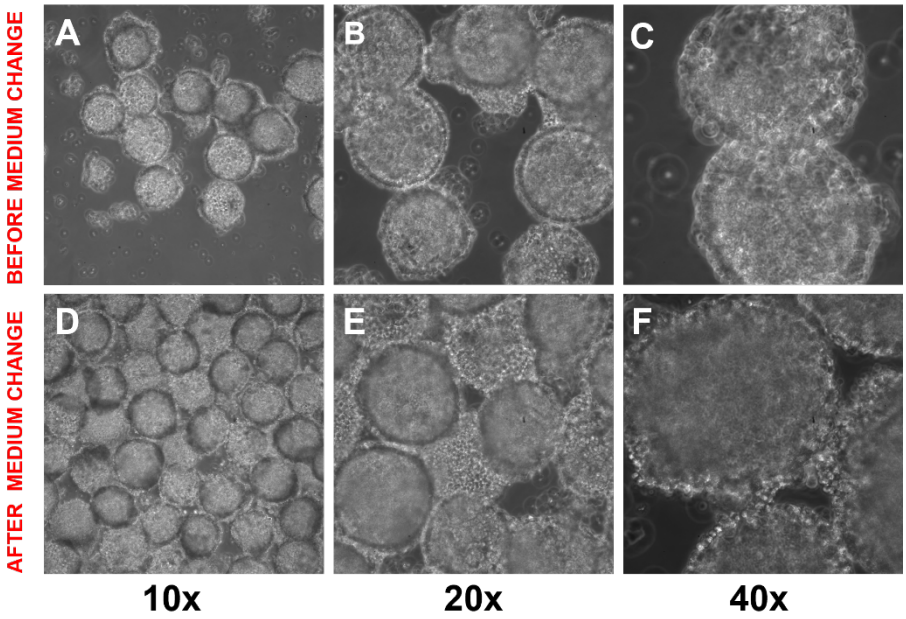

Figure 13. Representative images of growing cells on dissolvable microcarriers in the ultra-low attachment bacteriological Petri dish of 20 mm height (ii) inspected under the microscope before (**top panel**; **A**, **B**, **C**) and after changing the culture medium (**bottom panel**; **D**, **E**, **F**) at day 4 (96 hours following cell seeding). Images were acquired at 10x (**A**, **D**), 20x (**B**, **D**) and 40x (**C**, **F**) magnification.

Cell Harvest of RAW 264.7 cells grown on dissolvable microcarriers

RAW 264.7 cells in both ultra-low attachment bacteriological Petri dishes of 15 mm height (iii) along with those in one plate of a deep-form bacteriological Petri dish of 25 mm height (type i; Plate 2, indicated as NUNC) were harvested on day 4 (96 hours following cell seeding). The cells in the remaining two deep-form bacteriological Petri dishes of 25 mm height (type i; Plate 1 and 3) along with those in the ultra-low attachment bacteriological Petri dish of 20 mm height (ii) were harvested on day 5 (120 hours following cell seeding). Cells were harvested following the microcarrier dissolution achieved by adding a solution containing EDTA, which chelates calcium ions and destabilises the polymers crosslinking, and pectinase, responsible of PGA polymer degradation. The harvested solution was prepared by adding 1.32 ml of pectinase (Sigma Cat. No. P2611; 3800 U/ml) and 1 ml of 0.5 M EDTA (USB Corp. Cleveland No.15694) in 57.44 ml of 0.25% Trypsin / 0.25% EDTA in HBSS w/o Calcium & Magnesium.

To dissolve the microcarriers and harvest the cells, the same procedure was used for all plates. It consisted of removing the medium, washing two times the cells with 1x phosphate buffered saline (PBS), add the pre-warmed harvesting solution and stir suspension gently for 10 to 20 min. The only difference between the harvested cells on day 4 and day 5 consisted of the way used to allow the microcarriers to settle before removing the medium or PBS. On day 4, the microcarriers were settled by 1 min centrifugation at 200 x g, while on day 5 they were settled by waiting for ~5 to 10 min before removing the medium or PBS.

Fig. 14 shows the comparison between the images acquired on day 4 before proceeding to dissolve the microcarriers and cell harvest on both, ultra-low attachment bacteriological Petri dishes of 15 mm height (iii) (**top panel**, **A** – **C**, Plate 1; **middle panel**, **D** – **F**, Plate 2) and one deep-form bacteriological Petri dish of 25 mm height (i) (**bottom panel**, **G** – **I**, Plate 2 indicates as NUNC), and the corresponding images (**left column**, **J** – **L**) acquired 20 minutes after adding the harvesting solution. Before starting with the dissolution procedure to harvest the cells, each plate was inspected under the microscope and imaged at 10x (**A**, **D**, **G**), 20x (**B**, **E**, **H**), and 40x (**C**, **F**, **I**) magnification. When the microcarriers dissolution procedure was completed, each plate was inspected again under the microscope and imaged at 40x magnification (**left column**, **J** – **L**). For each plate, harvested cells were counted using the Trypan Blue exclusion assay. For Plate 1 and 2 of the ultra-low attachment bacteriological Petri dishes of 15 mm height (iii), the numbers of cells were respectively $28.86 \cdot 10^6$ and $27.60 \cdot 10^6$ while for the deep-form bacteriological Petri dish of 25 mm height (i) indicated as NUNC Plate 2 in **Fig. 14** resulted as $14.76 \cdot 10^6$. This lower number was due to an error in aspirating the culture medium on day 1 when microcarriers were barely visible, as previously addressed.

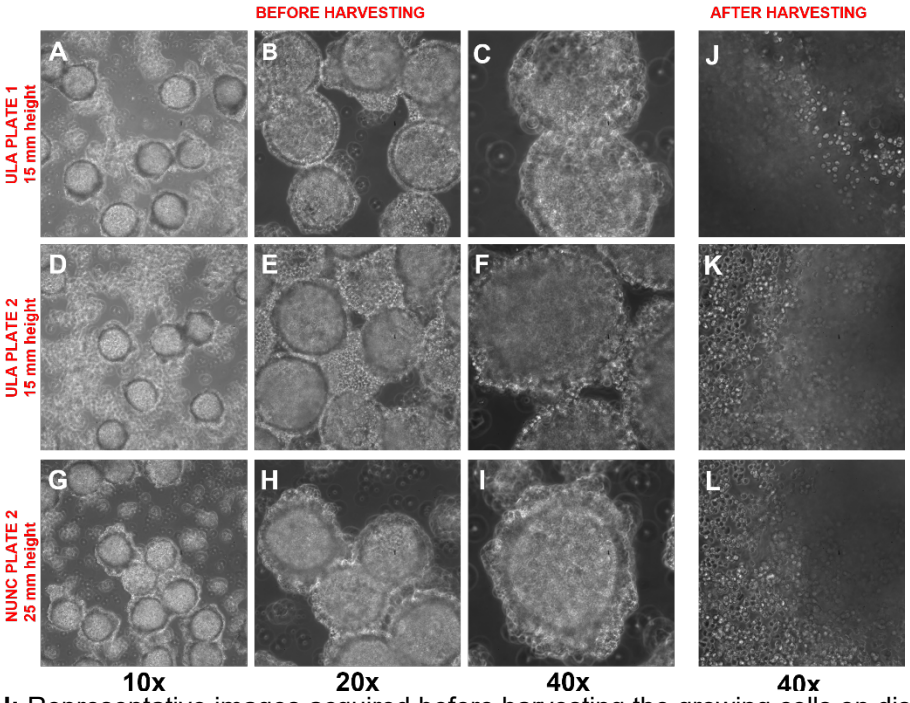

Figure 14. Right panel: Representative images acquired before harvesting the growing cells on dissolvable microcarriers in both ultra-low attachment bacteriological Petri dishes of 15 mm height (iii) (**top panel**, **A** – **C**, Plate 1; **middle panel**, **D** – **F**, Plate 2) and in one deep-form bacteriological Petri dish of 25 mm height (i), indicated as NUNC Plate 2 (**bottom panel**, **G** – **I**). **Left panel:** Images acquired 20 min after adding the harvested solution showing the microcarriers dissolution for each plate (**J** – **L**). During the dissolution procedure microcarriers were settled using the centrifuge for 1 min.

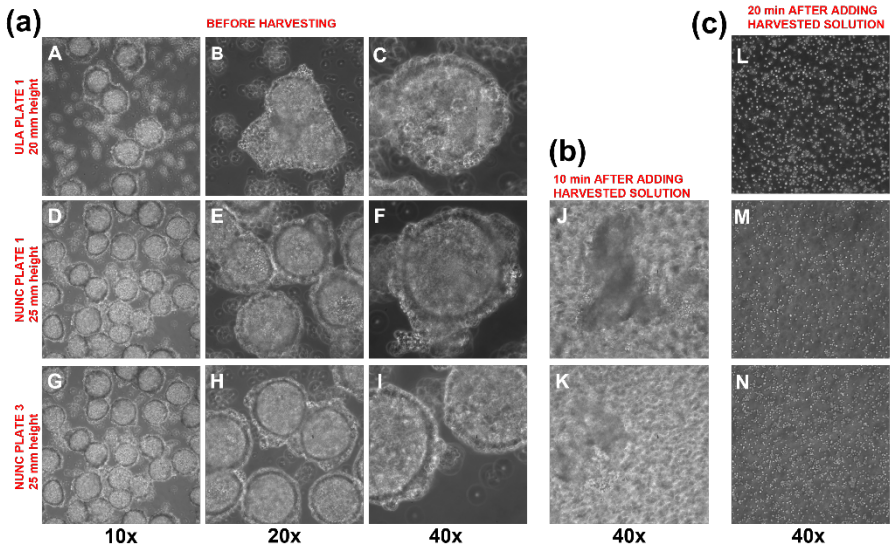

Figure 15. (**a**): Representative images acquired before dissolving the microcarriers in the ultra-low attachment bacteriological Petri dish of 20 mm height (ii) (**A** - **C**) and in the deep-form bacteriological Petri dishes of 25 mm height (i), (**middle panel**; **D** – **F**, NUNC Plate 1; **bottom panel**, **J** – **I**, NUNC Plate 3). (**b**): Images acquired 10 min after adding the harvested solution showing the dissolution state of microcarriers for NUNC Plate 1 (**J**) and NUNC Plate 3 (**K**). (**c**): Images acquired after adding the harvesting solution showing the microcarriers dissolution for each plate (**J** – **L**). During the dissolution procedure the microcarriers were settled by waiting for 5 up 10 min.

Fig. 15 (**a**) shows growing cells on dissolvable microcarriers at day 5 before dissolving the microcarriers. Images were acquired in the ultra-low attachment bacteriological Petri dish of 20 mm height (ii), indicated as ULA Plate 1 (**top panel**, **A** – **C**) and in the deep-form bacteriological Petri dishes of 25 mm height (i) (**middle panel**, **D** – **F**, NUNC Plate 1; **bottom panel, G** – **I**, NUNC Plate 3) with 10x (**A**, **D**, **G**), 20x (**B**, **E**, **H**), and 40x (**C**, **F**, **I**) magnification. In **Fig. 15** (**b**), images show the dissolution state of microcarriers in NUNC plate 1 (**J**) and NUNC plate 3 (**K**) 10 minutes after adding the harvested solution. **Fig. 15** (**c**), show the complete dissolution of microcarriers in ULA Plate 1 (**L**), NUNC Plate 1 (**M)** and NUNC Plate 3 (**N**) 20 min after adding

the harvested solution. Images in Fig. 15 (b) and (c) were acquired with 40x magnification. The number of live cells harvested in the ultra-low attachment bacteriological Petri dish of 20 mm height (ii) was $19.14 \cdot 10^6$. Cells harvested in both remaining deep-form bacteriological Petri dishes of 25 mm height (i), indicated as NUNC, were $24.46 \cdot 10^6$ and $22.47 \cdot 10^6$ for Plate 1 and 3, respectively.

Cell attachment on dissolvable microcarriers (response to pipetting)

To verify the solid attachment of RAW 264.7 cells on the dissolvable microcarriers, a sample of 2 ml growing cells on microcarriers was obtained from the ultra-low attachment bacteriological Petri dish of 20 mm height (ii) on day 5. Microcarriers were manually stimulated by pipetting with increasing strength from gently to very strong. After applying increasing strength, the sample was inspected under the microscope and imaged with 20x and 40x magnification, as shown in **Fig. 16**. Following an increased strength in the manual stimulation (pipetting), RAW 264.7 cells continued to be attached to the dissolvable microcarriers, even after applying a very strong stimulation (**Fig.16**). This indicates that RAW 264.7 cells are expected to remain attached to the dissolvable microcarriers during the loading into the perfusion system and subsequently continuously growing on them to allow the MRS monitoring of their metabolism, with and without treatment with DFP or other drugs.

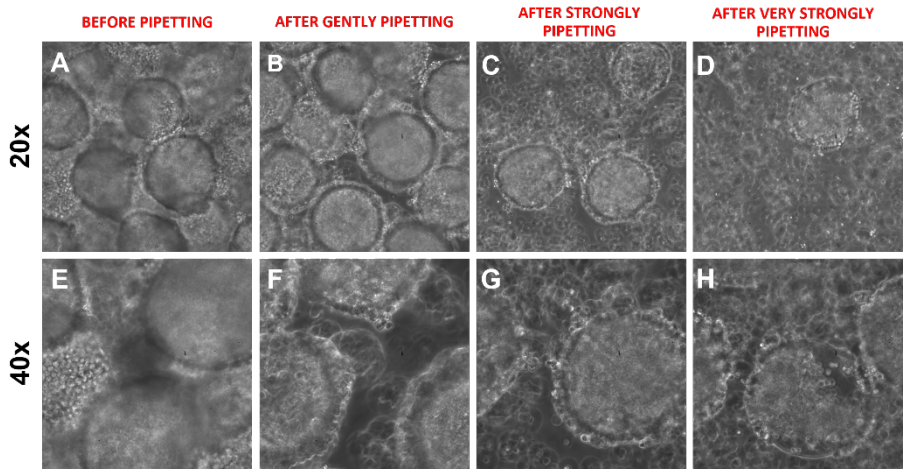

Figure 16. Representative images acquired on a sample of dissolvable microcarriers (2 ml) obtained from the ultra-low attachment bacteriological Petri dish of 20 mm height (ii) 5 days after cell seeding. Images were acquired before manually stimulating the microcarriers (**A**, **E**) and immediately after gently pipetting (**B**, **F**), strongly pipetting (**C**, **G**) and very strongly pipetting (**D**, **I**). For each different strength, images were acquired with 20x (**top panel**, **A** - **D**) and 40x (**bottom panel**, **E** - **H**) magnification.

Final considerations

As shown from the previous images, dissolvable microcarriers are appropriate for growing the RAW 264.7 cells and monitoring them with ^{31}P and ^{13}C MR spectroscopy using our MR-compatible bioreactor. As shown from **Fig. 16**, RAW 264.7 cells remain attached to the dissolvable microcarriers also after a very strong manual stimulation, indicating that they can very likely remain attached to the dissolvable microcarriers when loaded into the perfusion system and grow on them during the subsequent monitoring of their metabolism by MRS.

Fig. 3 and **Fig. 4** further show that it might not be necessary to change the medium 24 hours after the seeding. In addition, images acquired on the ultra-low attachment plates (ii; iii) (**Fig. 6**, **8**, **10**, **11**, **13**) compared with those acquired on the deep-form bacteriological Petri dishes (i) (**Fig. 5**, **7**, **9**, **12**) do not show substantial differences. Therefore, the use of the deep-form bacteriological Petri dishes of 25 mm height (i) appear more suitable, as their height eases their handling. Finally, **Fig. 12** and **Fig. 13** show that day 4 (96 hours following cell seeding) might be the best day for loading the cells on the perfusion system.

Section 5: Aim 1: Effect of DFP on Oxygen Consumption of Breast Tumor Cells and Macrophages (Koutcher and Merghoub/Blasberg laboratories)

The focus of oxygen consumption rate (OCR) measurements has been to measure the effect of DFP on triple negative breast tumor (TNBC) cells, specifically the effect of DFP on basal and maximal respiration as a measure of oxygen utilization and its possible relation to metabolism at the cellular level. As macrophages are an important part of the tumor stroma that play a significant role in tumor progression and regression, OCR measurements of a macrophage cell line were included in these experiments. In last year's report, we presented data on these studies but only had an n=3 and had focused on optimization and normalization experiments. We now present data with n=5 independent studies for MDA-231 (human TNBC), 4T1 (murine TNBC) as well as unpolarized and polarized RAW 264.7 cells (murine macrophages). Initially, we summarize our methodology for the convenience of the reviewers before summarizing the results.

Methods

We evaluated the mitochondrial response to Deferiprone (DFP), an iron chelator, in 2 triple negative breast cancer cell lines, the human MDA-MB-231 and murine 4T1, as well as a macrophage cell line RAW 264.7, polarized (M1, M2) and unpolarized (M0). We measured the oxygen consumption rate (OCR) using the Seahorse XF Cell Mito Stress Test Kit (Agilent, Santa Clara, CA) on a Seahorse XFe96 flux analyzer (Agilent), following the manufacturer's instructions. This assay assesses mitochondrial function by measuring in live cells the effects of the sequential exposure to Oligomycin (Oligo; inhibition of ATP synthase), Carbonyl cyanide-p-trifluoromethoxyphenylhydrazone (FCCP; protonophore, uncoupler of mitochondrial oxidative phosphorylation) and Rotenone & Antimycin A (Rot/AA; inhibition of mitochondrial complexes III & I respectively) on cellular OCR (Fig. 1A). From the OCR measurements, 8 quantitative parameters are derived (Fig. 1A): Non-mitochondrial oxygen consumption (Non-Mito OC), Basal Respiration (Basal Resp), Proton Leak, ATP Production (ATP Prod), Maximal Respiration (Max Resp), Spare Respiratory Capacity (SRC), % Spare Respiratory Capacity (% SRC), and % Coupling Efficiency (% CE).

All cell lines were cultured at 37 °C in 5% CO_2 in a humidified incubator using high-glucose Dulbecco's modified essential medium (DMEM HG), supplemented with 10% fetal calf serum, 100 U/ml Penicillin, 100 µg/ml Streptomycin and 2 mM glutamine, bringing the final glutamine concentration to 6 mM glutamine,. Based on previous data (1), a 48 h exposure time to 100 µM DFP (~EC_{90} for most cell lines) was chosen. Cells were seeded 1 day prior to DFP exposure on a Seahorse XF96 V3 PS Cell Culture Microplate (Agilent), specific plates facilitating the xFe96 analyzer measurements.

In last year's report, we summarized preliminary pilot experiments to optimize cell seeding densities and assay acquisition parameters. Final cell seeding numbers / well were 40k, 6k, 1.7k, and 7k for MDA-MB-231, RAW 264.7, untreated 4T1, and DFP-treated 4T1 respectively. An additional group of untreated, unpolarized RAW 264.7 at 4k seeding density was included to confirm that the observation of the lack of cell seeding density effect in RAW 264.7 cells, due to cell density saturation at time of the flux analyzer measurements for seeding densities above 6k cells, was not further seen. The RAW 264.7 cells were polarized to M2 by exposure to 20 ng/ml IL-4 for 48 h and to M1 by exposure to 100 ng/ml LPS for 48 h (>12 h exposure time for IL-4 or LPS are needed for significant polarization (data not shown)). The optimized acquisition parameters were 3 repeat measurements (cycles) / assay injection stage (Oligo, FCCP, and Rot/AA respectively), a 3 min mixing time and a 2 min measurement/cycle.

After the XFe96 flux analyzer measurements, the total cell number / well and the total cell number in the sensor area of the Seahorse flux analyzer measurements (centered ~55% of total well area) as well as total protein / well were measured to facilitate normalization of the OCR measurements in each single well. Well images depicting the cell layer (Fig. 1B) were acquired by using the direct cell counting protocol on a Celigo Imaging Cytometer (Nexcelom Bioscience, Lawrence, MA) with a customized Seahorse XFe96 plate layout. Total cell numbers for each entire well and the sensor area (area between the posts in the well) were obtained by adjusting the analysis parameters for each cell line separately, due to their differences in contrast and cell shape (Fig. 1B). Of note is that 4T1 cells have a tendency, when confluent, to come off and fold over at well edges, potentially confounding the cell count. Thus, counting cells in the sensor area only versus the entire well area alleviates the impact of an inhomogeneous cell distribution on the OCR curve normalization. Here,

this was overall less of an issue, as cells were – by design – all at high confluence (>80%) at the time of the Seahorse analyzer experiment. Total protein, historically considered the gold standard for normalization of OCR curves, was measured by Pierce™ BCA Protein Assay Kit (Thermo Fisher Scientific, Waltham, MA) as described previously (1,2). Total protein is assumed to be directly proportional to cell number. However, this might not be true for all cell lines and might differ between cells lines, as well as be affected by treatments. Hence, we also evaluated the normalization by cell number. As the sensor of the sensor plate covers only ~55% of the well area, normalizing the OCR to the cell number in that area would reflect most closely the true OCR value / cell, while normalization to total cell number / well allows the comparison to the total protein measurements and how well total protein and total cell number are related. Data are presented using the sensor region for normalization although data were analyzed by all three methods

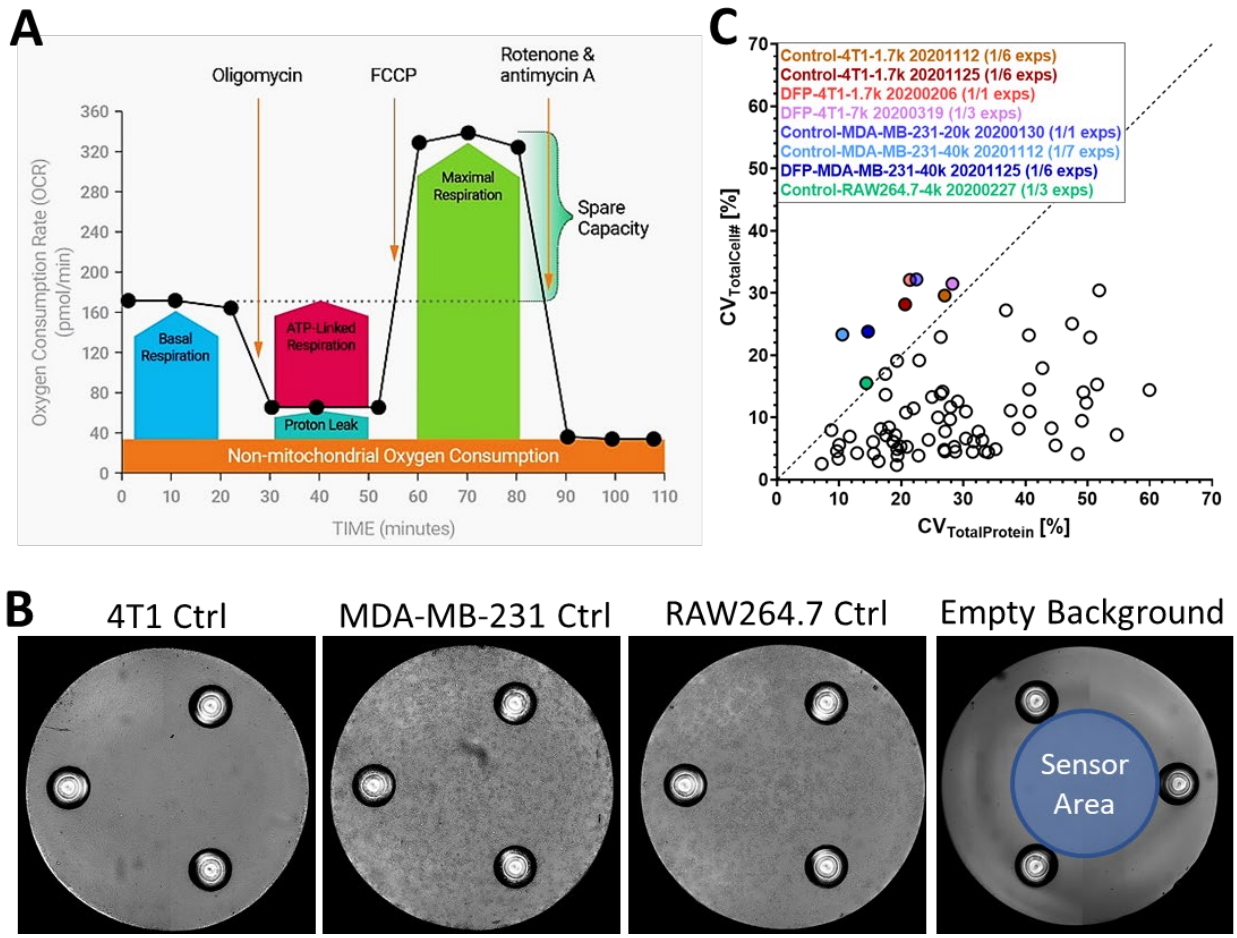

Figure 1: **(A)** Scheme of Cell Mito Stress Test and associated quantitative parameters calculated from each stage. The minimum OCR after Rot/AA injection delivers Non-Mito OC; the last rate measurement before Oligomycin injection is used to calculate the Basal Resp; the minimum OCR measurement after Oligo injection and maximum OCR measurement after FCCP injection are respectively used to calculate the remaining quantitative parameters. **(B)** Representative brightfield images of single wells with untreated cells of each cell type and an empty well. The 4 empty corner wells on the Seahorse plate serve as background controls for the Seahorse assay. The sensor area is a circular area within the three posts in each well. The differing contrast, cell density and growth homogeneity for each cell line can be discerned. **(C)** Total Protein measurements are overall more variable than Total Cell Counts. Each circle represents one experimental condition at one independent experiment with data derived from a total of 27 experimental conditions over 7 independent (separate) experiments, leading to a total of 78 different cohorts. Only 8 of the 78 cohorts (marked in color) have a smaller CV for Total Protein than for Total Cell Number. Only 3 of 78 cohorts had a similar (within < 1.5%) CV for Total Protein and Total Cell Number. (Data from 2 of 3 independent optimization experiments are included in this analysis. One optimization experiment had no cell count data, due to the Celigo imager being under repair.)

The Seahorse data were analyzed using the Wave 2 software (Agilent). For all wells, the OCR curves were visually inspected for experimental issues, such as defective loading of Oligo, FCCP, or Rot/AA and wells with loading issues at any of the 3 injection stages were excluded from further analysis. Some experiments had empty background wells, leading to unreliable background correction and distortion of Seahorse analyzer curves. We found that while the background correction had a large impact on the curves with improperly

treated, i.e. empty, background wells, the impact on the curves, and thus, the derived quantitative parameters was marginal in experiments with properly treated (non-empty) background wells. Hence, we analyzed the Seahorse analyzer curves for all experiments without the inbuilt background correction.

The OCR curves normalized by the three different normalizations and resulting 8 quantitative parameters were exported for further graphing and statistical analysis in GraphPad Prism 9 (GraphPad Software, LLC, San Diego, CA).

Statistical Analyses:

The statistical analysis was done separately for each normalization, i.e. data based on protein, total well cell counts and sensor area cell counts but we only present data based on sensor area cell number normalization.

To obtain for each quantitative parameter and each group the error of the mean averaged over all experiments, we propagated the SD of the mean from single experiments using the Gaussian error propagation, i.e. the square root of the sum of the squared single experiment SDs.

How TNBC cell type, macrophage polarization and/or exposure to DFP lead to significant differences in mitochondrial quantitative parameters between various groups was addressed by statistical comparisons. While a non-parametric analysis using the Friedman Test with Dunn's multiple comparison is the most rigorous statistical analysis, it significantly reduces the power to detect differences for comparably few (here 5) independent experimental repeats. As in each single experiment, there were anywhere from 4-10 (mostly 8) replicate wells for each of the 11 groups with very few outliers, and we repeated the experiment 5 times, we are confident of the intra- and interexperimental repeatability. Thus, we used a two-tailed, 1-way ANOVA with Geisser Greenhouse correction (intra-experimental group means paired by experiment date) followed by Bonferroni post hoc analysis to assess statistically significant differences of each mitochondrial quantitative parameter between groups.

Results and Discussion

As shown in last year's report and updated with the additional experiment for a total of n = 5 independent experiments, we compared 3 different normalizations of OCR curves and derived quantitative parameters: OCR curves normalized to (i) Total Protein, (ii) Total Cell Number, and (iii) Total Cell Number in Sensor Area. In agreement with last year's data, we found that total protein does not relate very well to total cell number at high density cultures (data not shown). Additionally, the total protein measurements had a higher coefficient of variation than the total cell number measurements (Fig. 1C). While the results across the different normalizations are comparable (data not shown), we will present the detailed results based on the normalization to the total cell number in the sensor area for the purpose of this report, as it most closely reflects the true OCR parameter for the cells

As each experiment contained 11 different groups, there are many potential comparisons. While including data for all quantitative parameters, we concentrate on the results for changes in basal and maximal respiration which were the focus of the initial application. We include tables with P values for each comparison grouping covering all quantitative parameters.

Figure 2 shows a typical result of normalized Seahorse analyzer curves from a single experiment for the 11 groups. For 4T1 and MDA-MB-231 cells, the normalized OCRs in the Rot/AA stage are similar between the respective untreated and DFP-exposed cells. That means that any differences visible in the BL (1st) stage of the curve can be attributed to differences in basal respiration, while the lowest values in the Oligo stage reflect H^+ Leak and ATP Prod changes, and the highest values in the FCCP stage reflect directly changes in maximal respiration and corresponding SRC. In RAW 264.7 cells, DFP leads to a lowering of the non-Mito OC in M1-polarized cells, while polarization per se and DFP exposure of M0 and M2 RAW 264.7 cells lead to only modest variations of the non-Mito OC as reflected in the Rot/AA stage of the curves.

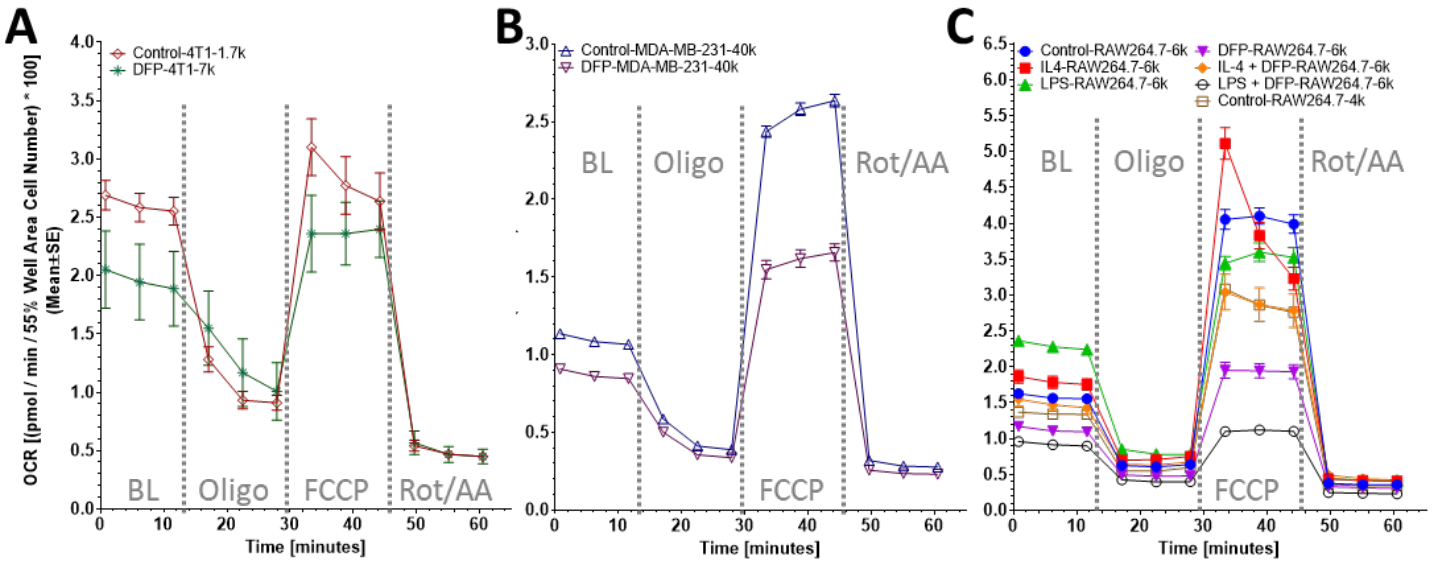

Figure 2: Oxygen Consumption Rates (OCRs) normalized to cell number in the sensor area of each well for either untreated or DFP-treated (**A**) murine TNBC cells 4T1 (n=10 Control; n = 5 DFP), (**B**) human TNBC cells MDA-MB-231 (n = 8 Control; n = 8 DFP), and (**C**) unpolarized and polarized RAW 264.7 cells (n = 8 control, except n = 7 for LPS-RAW264.7; n = 8 DFP). (**C**) also includes a RAW 264.7 cell number control. Representative data from 1 of 5 independent experiments.

The repeatability of the quantitative parameters within and across independent experiments, i.e. the intra-and inter-experimental variability, is demonstrated representatively for all 11 groups by basal respiration in Figure 3. For sensor area cell number normalization, group membership accounted for ~26.5% to ~58% of the Total Variance while experiment date which accounted between ~1% to ~7.4% of Total Variance across all 8 quantitative mitochondrial parameters (2-way ANOVA with Tukey multiple comparison test). Also, an interaction between groups and experiment date contributed significantly to the % Total Variance. Similarly, group membership, experiment date and their interaction were significant sources of variation for each quantitative parameter obtained from either total protein or total cell number normalization. Thus, all statistical analyses of quantitative parameters (and curves) were performed paired to experiment date. Excepting SRC and % SRC, intra-experimental variability increased for all other mitochondrial quantitative parameters with decreasing cell doubling time. That is MDA-MB231 cells with the longest cell doubling time had the lowest intraexperimental variability followed by RAW 264.7 cells and 4T1 cells as the cell doubling time decreases (Figure 3).

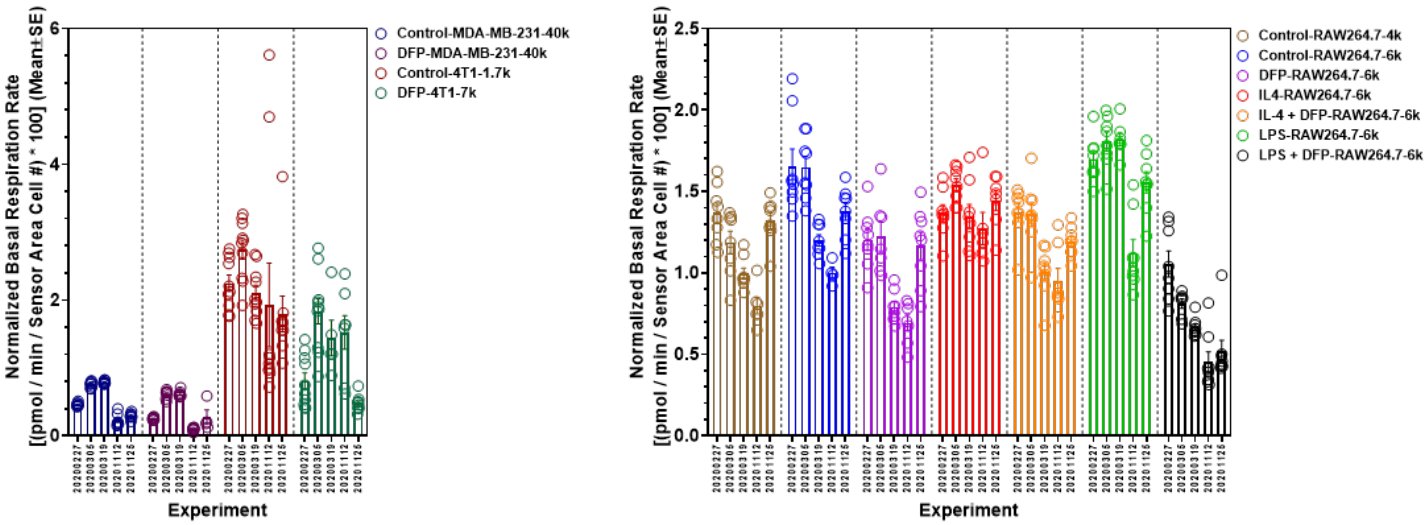

Figure 3: Inter- and intra-experimental variability of basal respiration of the 2 TNBC lines, untreated or DFP-treated (left panel) as well as unpolarized (M0), M1 (by LPS)- and M2 (by IL-4)-polarized RAW 264.7 cells. The bars display the mean±SE of separate experiments, while the open circles represent single wells within each experiment.

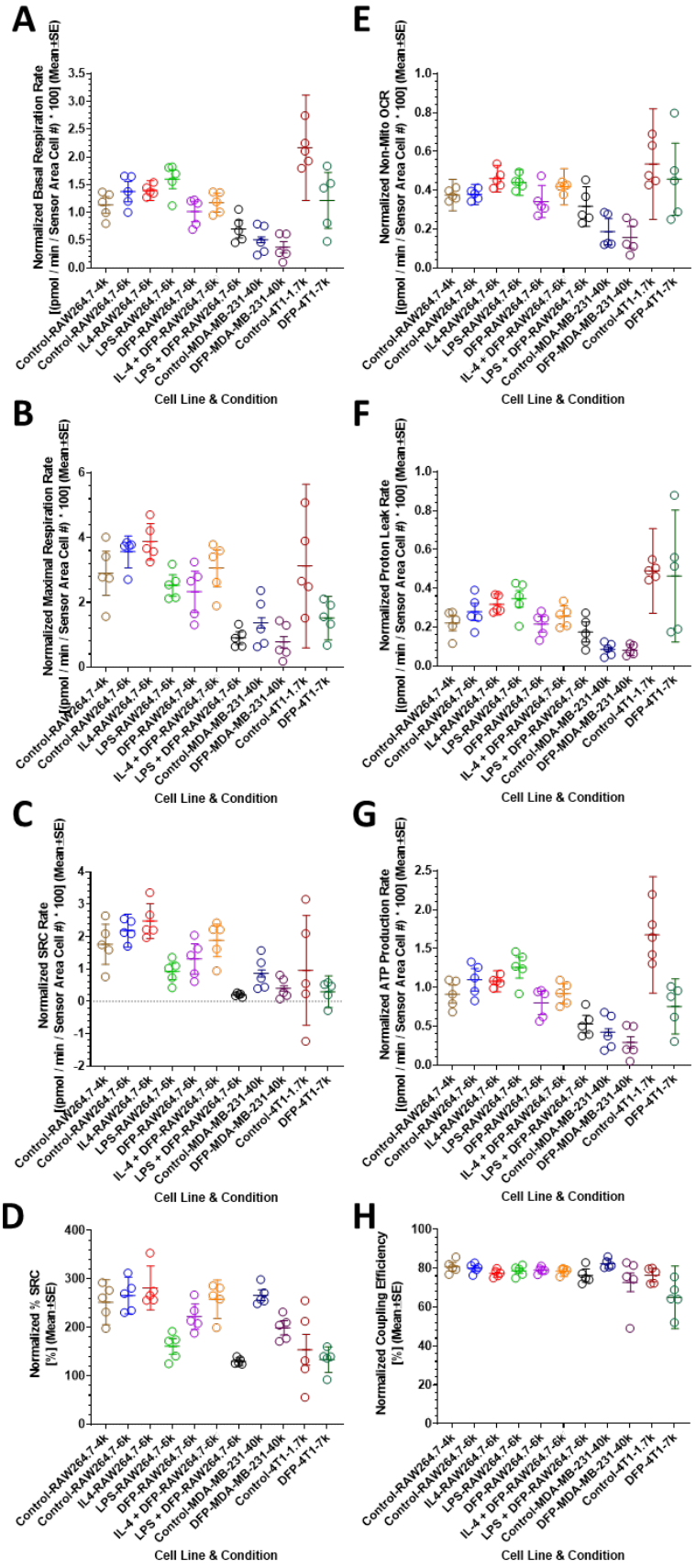

Figure 4: Quantitative mitochondrial parameters for the 11 experimental groups. **A-H** display single experiment means (open circles, n = 5) overlaid with the overall mean±SE for Basal Resp, Max Resp, SRC, % SRC, Non-Mito OC, H^+ Leak, ATP Prod, and % CE respectively. Overall SE was calculated by propagating the SD error of the means from each single experiment.

The summary graphs for the 8 quantitative mitochondrial parameters based on sensor area cell number normalization are shown for all experimental groups in Figure 4.

Table 1-5 list the P Values for the group comparisons based on various scientific inquiries, i.e. A) The comparison of 2 different TNBC cell types in the presence and absence of DFP, B) the effect of DFP on cancer cells or macrophages, C) the effect of polarization of macrophages in the presence and absence of DFP and D) the differences between unpolarized macrophages and TNBC cell lines in the absence and presence of DFP.

We found that human versus murine TNBC cells have very different mitochondrial parameters: Basal respiration (Fig. 4A), NonMito OC (Fig. 4E), H^+ Leak (Fig. 4F), and ATP Production (Fig. 4G) are significantly higher, with % Coupling Efficiency (Fig. 4H) significantly lower in untreated 4T1 than untreated MDA-MB-231 cells (Table 1, 2).

In DFP-exposed TNBC cells, the differences between 4T1 and MDA-MB-231 are reduced for basal respiration (Fig. 4A), H^+ Leak (Fig. 4F) and ATP Production (Fig. 4G), while % SRC (Fig. 4D) and NonMito OC (Fig. 4E) are respectively significantly lower and higher in DFP-treated 4T1 than DFP-treated MDA-MB-231 cells (Table 1, 2). This is consistent with the observed prolongation of the cell doubling time, i.e. reduced cell growth, in response to DFP.

DFP exposure of 4T1 cells reduces significantly their basal respiration and ATP production (Fig. 4 A, G and Table 1, 2). In MDA-MB-231 cells, DFP reduces significantly basal respiration, maximal respiration, ATP Production, SRC and %SRC (Figure 4, Table 1, 2).

These differences in mitochondrial parameter between the 2 TNBC cell lines and their response to DFP exposure are consistent with their differences in growth rates as well as their respective growth rate reductions in response to DFP. We hypothesize that a higher aerobic glycolysis in 4T1 cells than MDA-MB-231 cells contributes to these differences as well.

The observed TNBC DFP response agrees with our previous observation in 3 prostate cancer lines, where a 24 h exposure to DFP significantly diminished Basal Resp, Max Resp, H^+ Leak (in 2 of 3 cell lines), ATP Prod (in 2 of 3 cell lines), and SRC (in 2 of 3 cell lines), while not affecting NonMitoOC [9].

Table 1: Statistical analysis to assess the differences of NonMito OC, Basal Resp, and Max Resp between the human and murine TNBC line and the effects of DFP exposure on either. Uncorrected P values (Fisher's LSD test) color coded for Bonferroni correction, based on multiple comparison group size n to achieve 95% significance: n =1, **P ≤ 0.05**; n = 2, **P ≤ 0.025**; n = 3, **P ≤ 0.0167**; n = 4, **P ≤ 0.0125**; n = 5, **P ≤ 0.01**.

TNBC Cell Line Differences in the Presence and Absence of DFP		
	NonMito OC	Basal Resp	Max Resp
Control-4T1-1.7k *vs.* Control-MDA-MB-231-40k	**0.0055**	**0.0001**	0.1245
DFP-4T1-7k *vs.* DFP-MDA-MB-231-40k	**0.0199**	**0.0401**	0.0722
Effect of 48 h DFP Exposure on a Human and a Murine TNBC Cell Line		
	NonMito OC	Basal Resp	Max Resp
DFP-4T1-7k *vs.* Control-4T1-1.7k	0.3436	**0.0083**	0.0652
DFP-MDA-MB-231-40k *vs.* Control-MDA-MB-231-40k	0.0531	**0.0125**	**0.0057**

Table 2: Statistical analysis to assess the differences of H^+ Leak, ATP Prod, SRC, % SRC and % CE between the human and murine TNBC line and the effects of DFP exposure on either. Uncorrected P values (Fisher's LSD test) color coded for Bonferroni correction, based on multiple comparison group size n to achieve 95% significance: n =1, **P ≤ 0.05**; n = 2, **P ≤ 0.025**; n = 3, **P ≤ 0.0167**; n = 4, **P ≤ 0.0125**; n = 5, **P ≤ 0.01**.

TNBC Cell Line Differences in the Presence and Absence of DFP					
	H^+ Leak	ATP Prod	SRC	% SRC	% CE
Control-4T1-1.7k *vs.* Control-MDA-MB-231-40k	**<0.0001**	**0.0004**	0.9213	**0.0373**	**0.0215**
DFP-4T1-7k *vs.* DFP-MDA-MB-231-40k	**0.0359**	**0.0294**	0.6998	**0.0199**	0.4104
Effect of 48 h DFP Exposure on a Human and a Murine TNBC Cell Line					
	H^+ Leak	ATP Prod	SRC	% SRC	% CE
DFP-4T1-7k *vs.* Control-4T1-1.7k	0.8347	**0.0038**	0.3798	0.557	0.0619
DFP-MDA-MB-231-40k *vs.* Control-MDA-MB-231-40k	0.6243	**0.0065**	**0.0063**	**0.0015**	0.1641

The mitochondrial parameter values for unpolarized and polarized RAW 264.7 cells tend to fall in between the corresponding parameter values observed for the TNBC cell lines (Fig. 4).

In RAW 264.7 cells, DFP exposure significantly reduces basal respiration and ATP production, independent of polarization, while maximal respiration, proton leak, and SRC were significantly affected in M0 and M1-polarized RAW 264.7 cells (Figure 4, Table 3, 4). M1 (by LPS)-polarized RAW 264.7 cells were the most sensitive to DFP and displayed significantly reduced NonMito OC in response to DFP. This sensitivity to DFP parallels the observation in Section 1 of this report where M1-polarized RAW 264.7 cells release the highest phagocytosis and release the highest amount of NO in response to DFP (Section 1, Figure 2). Of note is also that not all RAW 264.7 cells are polarized in cultures exposed to 48 h of IL-4 and LPS respectively. As described in Section 1, Figure 1 of this report, approximately 60-70% of untreated and DFP-treated RAW 264.7 cells are M2 polarized, while ~26% in untreated and ~37% in DFP-treated RAW 264.7 are M1 polarized as a result of exposure to IL-4 and LPS respectively.

Exposure of the 2 TNBC lines as well as unpolarized and M2-polarized RAW 264.7 cells to 100 μM DFP, did not significantly affect NonMito OC (Fig. 4B, Table 1, 3), consistent with the iron chelation effect on mitochondrial, iron-dependent enzymes and corresponding effect on cell proliferation (see also Section 2, Figure 2. (2).

The M1 (LPS) polarization of RAW 264.7 cells reduced maximal respiration, SRC, and % SRC in the presence and absence of DFP, with basal respiration and ATP production lower in the presence and not absence of

DFP, compared to unpolarized and M2-polarized RAW 264.7 cells (Fig. 4, Table 3, 4). In the presence of DFP, M2 (by IL-4) polarization of RAW 264.7 cells decreases the basal respiration, maximal respiration, proton leak, ATP Production, and SRC compared to unpolarized RAW 264.7 cells (Fig. 4, Table 3, 4). These observations are consistent with the findings by others that M1 macrophages typically feature increased pentose phosphate pathway and glycolytic fluxes, supplemented by a dysfunctional Krebs (TCA) cycle (3,4). Due to the impaired reactions catalyzed by isocitrate dehydrogenase and succinate dehydrogenase, citrate and succinate accumulate in M1 macrophages (3,4). The higher ATP production of M1 RAW 264.7 cells in the absence of DFP compared to M0- and M2-polarized RAW 264.7 cells is reflective of ATP preferentially derived from glucose. The higher reliance of M0 and M2 macrophages on the Krebs cycle agrees with their higher Max Resp, SRC, and % SRC compared to M1 macrophages. The lower % SRC (Max Resp / Basal Resp) in M1 than in M2 macrophages might be the result of their reliance on the faster glycolysis and some modest increase in OXPHOS, similar to what has been observed in other studies(5) [13]. Taken together, this would also explain why M1 macrophages are more strongly impacted by DFP which inhibits aconitase in the TCA cycle and results in further accumulation of citrate and inhibition of TCA cycle, similar to our observation in prostate cancer (1).

Table 3: Statistical analysis to assess the effects of DFP on NonMito OC, Basal Resp, and Max Resp of unpolarized and polarized macrophages as well as the effects of macrophage polarization in the presence and absence of DFP. Uncorrected p values (Fisher's LSD test) color coded for Bonferroni correction, based on multiple comparison group size to achieve 95% significance: n =1, **P ≤ 0.05**; n = 2, **P ≤ 0.025**; n = 3, **P ≤ 0.0167**; n = 4, **P ≤ 0.0125**; n = 5, **P ≤ 0.01**.

Effect of 48 h DFP Exposure on Unpolarized and Polarized Macrophages			
	NonMito OC	Basal Resp	Max Resp
DFP-RAW264.7-6k *vs.* Control-RAW264.7-6k	0.3349	**0.0012**	**0.0091**
LPS + DFP-RAW264.7-6k *vs.* LPS-RAW264.7-6k (M1)	**0.0144**	**0.001**	**0.0031**
IL-4 + DFP-RAW264.7-6k *vs.* IL4-RAW264.7-6k (M2)	0.1215	**0.0242**	0.1043
Effect of Macrophage Polarization in the Absence of DFP			
	NonMito OC	Basal Resp	Max Resp
IL4-RAW264.7-6k *vs.* Control-RAW264.7-6k	0.0565	0.8622	0.2257
LPS-RAW264.7-6k *vs.* Control-RAW264.7-6k	0.0529	0.0919	**0.0075**
LPS-RAW264.7-6k *vs.* IL4-RAW264.7-6k	0.3633	0.1255	**0.0004**
Effect of Macrophage Polarization in the Presence of DFP			
	NonMito OC	Basal Resp	Max Resp
IL-4 + DFP-RAW264.7-6k *vs.* DFP-RAW264.7-6k	0.0693	**0.0148**	**0.0067**
LPS + DFP-RAW264.7-6k *vs.* DFP-RAW264.7-6k	0.1973	**0.0321**	**0.0092**
LPS + DFP-RAW264.7-6k *vs.* IL-4 + DFP-RAW264.7-6k	**0.048**	**0.0021**	**0.0018**

Table 4: Statistical analysis to assess the effects of DFP on H^+ Leak, ATP Prod, SRC, and % SRC of unpolarized and polarized macrophages as well as the effects of macrophage polarization in the presence and absence of DFP. Uncorrected p values (Fisher's LSD test) color coded for Bonferroni correction, based on multiple comparison group size to achieve 95% significance: n =1, **P ≤ 0.05**; n = 2, **P ≤ 0.025**; n = 3, **P ≤ 0.0167**; n = 4, **P ≤ 0.0125**; n = 5, **P ≤ 0.01**.

Effect of 48 h DFP Exposure on Unpolarized and Polarized Macrophages					
	H^+ Leak	ATP Prod	SRC	% SRC	% CE
DFP-RAW264.7-6k *vs.* Control-RAW264.7-6k	**0.0221**	**0.0005**	**0.0306**	0.146	0.1204
LPS + DFP-RAW264.7-6k *vs.* LPS-RAW264.7-6k	**0.0003**	**0.0013**	**0.0142**	**0.0397**	0.1201
IL-4 + DFP-RAW264.7-6k *vs.* IL4-RAW264.7-6k	**0.0352**	**0.0243**	0.1552	0.368	0.1646

Effect of Macrophage Polarization in the Absence of DFP					
	H^+ Leak	ATP Prod	SRC	% SRC	% CE
IL4-RAW264.7-6k *vs.* Control-RAW264.7-6k	0.3185	0.7923	0.1782	0.3388	0.1187
LPS-RAW264.7-6k *vs.* Control-RAW264.7-6k	**0.0173**	0.1686	**0.0015**	**0.0005**	0.3019
LPS-RAW264.7-6k *vs.* IL4-RAW264.7-6k	0.5288	0.0793	**0.002**	**0.0043**	0.5009
Effect of Macrophage Polarization in the Presence of DFP					
	H^+ Leak	ATP Prod	SRC	% SRC	% CE
IL-4 + DFP-RAW264.7-6k *vs.* DFP-RAW264.7-6k	**0.0073**	**0.023**	**0.0173**	0.0528	0.3006
LPS + DFP-RAW264.7-6k *vs.* DFP-RAW264.7-6k	0.1954	**0.0206**	**0.0119**	**0.0043**	0.1021
LPS + DFP-RAW264.7-6k *vs.* IL-4 + DFP-RAW264.7-6k	**0.0332**	**0.0008**	**0.0033**	**0.0022**	0.2824

Unpolarized, untreated RAW 264.7 cells have a significantly lower basal respiration, proton leak, and ATP production than untreated 4T1 cells and a significantly higher basal respiration, proton leak, and ATP production than untreated MDA-MB-231 cells (Table 5). These differences are maintained in DFP exposed cells for MDA-MB-231 but not 4T1 cells (Fig. 4, Table 5). Maximal respiration and SRC (and to a lesser extent % SRC) are lower in untreated MDA-MB-231 cells than RAW 264.7 cells; a similar pattern is observed for DFP-treated cells (Fig. 4, Table 5). In the presence of DFP, unpolarized RAW 264.7 cells have a higher NonMito OC than MDA-MB-231 cells. In the presence of DFP, 4T1 cells have a lower % SRC and % CE than unpolarized RAW 264.7 cells Fig. 4, Table 5).

Table 5: Statistical analysis to assess the differences between unpolarized macrophages and TNBC cells in the presence and absence of DFP on NonMito OC, Basal Resp, Max Resp, H^+ Leak, ATP Prod, SRC, % SRC, and % CE. Uncorrected p values (Fisher's LSD test) color coded for Bonferroni correction, based on multiple comparison group size to achieve 95% significance: n =1, **P ≤ 0.05**; n = 2, **P ≤ 0.025**; n = 3, **P ≤ 0.0167**; n = 4, **P ≤ 0.0125**; n = 5, **P ≤ 0.01**.

Effect of Macrophage and TNBC Cell Line Differences in the Absence and Presence of DFP				
	NonMito OC	Basal Resp	Max Resp	H^+ Leak
Control-4T1-1.7k *vs.* Control-RAW264.7-6k	0.0607	**0.003**	0.6101	**0.0047**
Control-MDA-MB-231-40k *vs.* Control-RAW264.7-6k	**0.0118**	**0.0031**	**0.0018**	**0.0019**
DFP-4T1-7k *vs.* DFP-RAW264.7-6k	0.2128	0.5492	0.2348	0.1359
DFP-MDA-MB-231-40k *vs.* DFP-RAW264.7-6k	**0.0027**	**0.0095**	**0.0253**	**0.0065**
Effect of Macrophage and TNBC Cell Line Differences in the Absence and Presence of DFP				
	ATP Prod	SRC	% SRC	% CE
Control-4T1-1.7k *vs.* Control-RAW264.7-6k	**0.0097**	0.209	**0.0243**	0.2545
Control-MDA-MB-231-40k *vs.* Control-RAW264.7-6k	**0.0049**	**0.0025**	0.9593	0.291
DFP-4T1-7k *vs.* DFP-RAW264.7-6k	0.8237	**0.0397**	**0.0024**	**0.0127**
DFP-MDA-MB-231-40k *vs.* DFP-RAW264.7-6k	**0.012**	**0.0433**	0.2482	0.4002

In summary, cell type impacted the quantity of the 8 mitochondrial parameters with human TNBC cell line having typically the lowest values. DFP reduced basal respiration and maximal respiration (less so for 4T1) in the TNBC lines, consistent with our previous observations in prostate cancer cell lines. The results for the unpolarized and polarized RAW 264.7 cells reflect the induction of metabolic shifts between TCA cycle, glycolysis, and pentose phosphate pathway in response to intracellular iron chelation and/or macrophage polarization.

References

1. Simoes, R.V., et al., *Inhibition of prostate cancer proliferation by Deferiprone.* NMR Biomed, 2017. **30**(6).

2. Simoes, R.V., et al., *Metabolic plasticity of metastatic breast cancer cells: adaptation to changes in the microenvironment.* Neoplasia, 2015. **17**(8): p. 671-84.
3. Thapa, B. and K. Lee, *Metabolic influence on macrophage polarization and pathogenesis.* BMB Rep, 2019. **52**(6): p. 360-372.
4. Viola, A., et al., *The Metabolic Signature of Macrophage Responses.* Front Immunol, 2019. **10**: p. 1462.
5. Zuo, H. and Y. Wan, *Metabolic Reprogramming in Mitochondria of Myeloid Cells.* Cells, 2019. **9**(1).

What opportunities for training and professional development has the project provided?

If the project was not intended to provide training and professional development opportunities or there is nothing significant to report during this reporting period, state "Nothing to Report."

Describe opportunities for training and professional development provided to anyone who worked on the project or anyone who was involved in the activities supported by the project. "Training" activities are those in which individuals with advanced professional skills and experience assist others in attaining greater proficiency. Training activities may include, for example, courses or one-on-one work with a mentor. "Professional development" activities result in increased knowledge or skill in one's area of expertise and may include workshops, conferences, seminars, study groups, and individual study. Include participation in conferences, workshops, and seminars not listed under major activities.

This was not a training grant so there is nothing to report. Nevertheless, in Year 1 this supported Dr. Leftin who went on to write his own peer reviewed funding based on experiments begun under the auspices of this proposal and subsequently joined the faculty at SUNY Stony Brook. He used his training on iron studies and metabolism to advance to a full-time tenure track position. Dr. Porcari has been working on this project and is a postdoctoral fellow and has gone to three conferences to present findings from this project.

How were the results disseminated to communities of interest?

If there is nothing significant to report during this reporting period, state "Nothing to Report."
Describe how the results were disseminated to communities of interest. Include any outreach activities that were undertaken to reach members of communities who are not usually aware of these project activities, for the purpose of enhancing public understanding and increasing interest in learning and careers in science, technology, and the humanities.

1. Porcari, P., **Ackerstaff, E.**, LeKaye, H.C., Koutcher, J.A. *Metabolic Effects of Deferiprone on Triple Negative Breast Cancer.* Digital Poster #1843, 29th Ann Mtg & Exhibit of the International Soc for Magn Reson in Med (ISMRM), ISMRM & SMRT, Virtual Conference & Exhibition, May 15 – 20, 2021.
2. Porcari P, Ackerstaff E, Winkleman DP, Veeraperumal S, Kruchevsky N, Lekaye HC, Koutcher JA. **The Role of Iron Chelation in the Tumour Microenvironment of Triple-Negative Breast Cancer**. 28th ISMRM Annual Meeting, Virtual Conference 2020, August 8-14. Oral Presentation, 0144. (selected for presentation at the **Cancer Imaging Highlights Sessions** of the ISMRM 2020).
3. "Iron Chelation Affects Cell Growth and Metabolism in the Triple-negative Breast Cancer Cell Line 4T1" Porcari P, LeKaye HC, Koutcher JA, Ackerstaff E. World Molecular Imaging Congress 2019, September 4-7, Montreal, Canada. Poster presentation, P300

What do you plan to do during the next reporting period to accomplish the goals?

If this is the final report, state "Nothing to Report."
Describe briefly what you plan to do during the next reporting period to accomplish the goals and objectives.

1. The effect of DFP on enhancing efficacy of PD-1 antibodies in vivo (**Koutcher Lab**) (data being analyzed currently)
2. The effect of DFP on MDA-MB-231 on tumor growth delay, as a single agent and in combination with cisplatin and paclitaxel (**Koutcher Lab**) (Data being analyzed currently)

4. **IMPACT:** D*escribe distinctive contributions, major accomplishments, innovations, successes, or any change in practice or behavior that has come about as a result of the project relative to:*

What was the impact on the development of the principal discipline(s) of the project?
If there is nothing significant to report during this reporting period, state "Nothing to Report."

Describe how findings, results, techniques that were developed or extended, or other products from the project made an impact or are likely to make an impact on the base of knowledge, theory, and research in the principal disciplinary field(s) of the project. Summarize using language that an intelligent lay audience can understand (Scientific American style).

In view of the fact that DFP is in clinical use, our most significant finding was that it enhanced immune response in the 4T1 murine TNBC, a tumor that is known to be immunologically "cold" (relatively inactive). We found that in the spleen 1) DFP increased the percent of CD4 and CD8 effector T cells, 2) enhanced these cell numbers when used in combination with cisplatin, 3) decreased cells that expressed high level of the inhibitory PD-1 receptor, indicating a shift to a pro-inflammatory environment, and a decrease in immune suppressive cells. In both spleen and tumor, DFP induced an increase in the ability of CD4 and CD8 T cells to make both IFNγ or TNFα, a marker of polyfunctionality in T cells. DFP induced an increase in macrophage cells that made either IFNγ or TNFα. DFP enhanced the efficiency of phagocytosis by RAW 264.7 cells. This effect was significant in all the culture conditions ($p = 0.0004$ for Control, $p = 0.0007$ for IL-4, $p = 0.0045$ for LPS) but most prominent in the LPS-treated group. In DFP-exposed TNBC cells, the differences between 4T1 and MDA-MB-231 are reduced for basal respiration, H^+ Leak, and ATP Production). This is consistent with the observed prolongation of the cell doubling time, i.e. reduced cell growth, in response to DFP. DFP exposure of 4T1 cells reduces significantly their basal respiration and ATP production. In MDA-MB-231 cells, DFP reduces significantly basal respiration, maximal respiration, ATP Production, SRC and %SRC. These differences in mitochondrial parameter between the 2 TNBC cell lines and their response to DFP exposure are consistent with their differences in growth rates as well as their respective growth rate reductions in response to DFP. These data suggest possible implications for developing treatment with drugs that inhibit energy production and indicate that sensitivity may depend on growth rate

What was the impact on other disciplines?
If there is nothing significant to report during this reporting period, state "Nothing to Report."

Describe how the findings, results, or techniques that were developed or improved, or other products from the project made an impact or are likely to make an impact on other disciplines.

Nothing to report

What was the impact on technology transfer?
If there is nothing significant to report during this reporting period, state "Nothing to Report."

Describe ways in which the project made an impact, or is likely to make an impact, on commercial technology or public use, including:

- *transfer of results to entities in government or industry;*
- *instances where the research has led to the initiation of a start-up company; or*
- *adoption of new practices.*

Nothing to report

What was the impact on society beyond science and technology?
If there is nothing significant to report during this reporting period, state "Nothing to Report."

Describe how results from the project made an impact, or are likely to make an impact, beyond the bounds of science, engineering, and the academic world on areas such as:

- *improving public knowledge, attitudes, skills, and abilities;*
- *changing behavior, practices, decision making, policies (including regulatory policies), or social actions; or*
- *improving social, economic, civic, or environmental conditions.*

In year 2, we have shown that MRI can be used to measure and quantitate iron in vivo. This MAY go to clinical use (**Koutcher Lab**). Otherwise, nothing to report.

5. CHANGES/PROBLEMS: *The PD/PI is reminded that the recipient organization is required to obtain prior written approval from the awarding agency grants official whenever there are significant changes in the project or its direction. If not previously reported in writing, provide the following additional information or state, "Nothing to Report," if applicable:*

Changes in approach and reasons for change
Describe any changes in approach during the reporting period and reasons for these changes. Remember that significant changes in objectives and scope require prior approval of the agency.

We present a lengthy study to develop methods of keeping cells alive in a perfusion apparatus which maybe relevant to other investigations (study 4 above). We have also investigated an additional tumor model since our preliminary in vivo results were disappointing which will be shared in the final report

Actual or anticipated problems or delays and actions or plans to resolve them
Describe problems or delays encountered during the reporting period and actions or plans to resolve them.

COVID-19 had a major impact. The laboratories were shut down for two months and a key person was stuck overseas. Fortunately, she had a computer and data to analyze but being away 6 months was a major loss to this project. Thus, the analysis of the metabolism studies on MDA-MB-231 which where the data were acquired in 12/19-3/20 were just completed and not truly digested in terms of biochemical significance. These data are being written up and a manuscript is almost complete.

Changes that had a significant impact on expenditures
Describe changes during the reporting period that may have had a significant impact on expenditures, for example, delays in hiring staff or favorable developments that enable meeting objectives at less cost than anticipated.

Loss of technician in year 2 for about 8 months has allowed us to carry funds over to a no cost extension year. Gap in postdoctoral fellows due to recruiting an experienced person from overseas has also allowed carry over of funds which is necessary to complete the studies due to these delays.

Significant changes in use or care of human subjects, vertebrate animals, biohazards, and/or select agents
Describe significant deviations, unexpected outcomes, or changes in approved protocols for the use or care of human subjects, vertebrate animals, biohazards, and/or select agents during the reporting period. If required, were these changes approved by the applicable institution committee (or equivalent) and reported to the agency? Also specify the applicable Institutional Review Board/Institutional Animal Care and Use Committee approval dates.

Significant changes in use or care of human subjects

No human subjects

Significant changes in use or care of vertebrate animals

No change in vertebrate animals

Significant changes in use of biohazards and/or select agents

None

6. PRODUCTS: *List any products resulting from the project during the reporting period. If there is nothing to report under a particular item, state "Nothing to Report."*

- **Publications, conference papers, and presentations**
  Report only the major publication(s) resulting from the work under this award.

1. Porcari, P., **Ackerstaff, E.**, LeKaye, H.C., Koutcher, J.A. *Metabolic Effects of Deferiprone on Triple Negative Breast Cancer.* Digital Poster #1843, 29th Ann Mtg & Exhibit of the International Soc for Magn Reson in Med (ISMRM), ISMRM & SMRT, Virtual Conference & Exhibition, May 15 – 20, 2021.
2. Porcari P, Ackerstaff E, Winkleman DP, Veeraperumal S, Kruchevsky N, Lekaye HC, Koutcher JA. **The Role of Iron Chelation in the Tumour Microenvironment of Triple-Negative Breast Cancer**. 28th ISMRM Annual Meeting, Virtual Conference 2020, August 8-14. Oral Presentation, 0144. (selected for presentation at the **Cancer Imaging Highlights Sessions** of the ISMRM 2020).
3. "Iron Chelation Affects Cell Growth and Metabolism in the Triple-negative Breast Cancer Cell Line 4T1" Porcari P, LeKaye HC, Koutcher JA, Ackerstaff E. World Molecular Imaging Congress 2019, September 4-7, Montreal, Canada. Poster presentation, P300

Journal publications. *List peer-reviewed articles or papers appearing in scientific, technical, or professional journals. Identify for each publication: Author(s); title; journal; volume: year; page numbers; status of publication (published; accepted, awaiting publication; submitted, under review; other); acknowledgement of federal support (yes/no).*

None during this period.

Books or other non-periodical, one-time publications. *Report any book, monograph, dissertation, abstract, or the like published as or in a separate publication, rather than a periodical or series. Include any significant publication in the proceedings of a one-time conference or in the report of a one-time study, commission, or the like. Identify for each one-time publication: author(s); title; editor; title of collection, if applicable; bibliographic information; year; type of publication (e.g., book, thesis or dissertation); status of publication (published; accepted, awaiting publication; submitted, under review; other); acknowledgement of federal support (yes/no).*

None.

Other publications, conference papers and presentations. *Identify any other publications, conference papers and/or presentations not reported above. Specify the status of the publication as noted above. List presentations made during the last year (international, national, local societies, military meetings, etc.). Use an asterisk (*) if presentation produced a manuscript.*

None.

- **Website(s) or other Internet site(s)**
  List the URL for any Internet site(s) that disseminates the results of the research activities. A short description of each site should be provided. It is not necessary to include the publications already specified above in this section.

None.

- **Technologies or techniques**
  Identify technologies or techniques that resulted from the research activities. Describe the technologies or techniques were shared.

None in Year 4.

- **Inventions, patent applications, and/or licenses**
  Identify inventions, patent applications with date, and/or licenses that have resulted from the research. Submission of this information as part of an interim research performance progress report is not a substitute for any other invention reporting required under the terms and conditions of an award.

None in Year 4.

- **Other Products**

  Identify any other reportable outcomes that were developed under this project. Reportable outcomes are defined as a research result that is or relates to a product, scientific advance, or research tool that makes a meaningful contribution toward the understanding, prevention, diagnosis, prognosis, treatment and /or rehabilitation of a disease, injury or condition, or to improve the quality of life. Examples include:

  - *data or databases;*
  - *physical collections;*
  - *audio or video products;*
  - *software;*
  - *models;*
  - *educational aids or curricula;*
  - *instruments or equipment;*
  - *research material (e.g., Germplasm; cell lines, DNA probes, animal models);*
  - *clinical interventions;*
  - *new business creation; and*
  - *other.*

None

7. PARTICIPANTS & OTHER COLLABORATING ORGANIZATIONS

What individuals have worked on the project?

Provide the following information for: (1) PDs/PIs; and (2) each person who has worked at least one person month per year on the project during the reporting period, regardless of the source of compensation (a person month equals approximately 160 hours of effort). If information is unchanged from a previous submission, provide the name only and indicate "no change".

Participants:

Koutcher Laboratory; W81XWH-17-1-0525 (Initiating PI)

Jason Koutcher; Corresponding PI, 9.3% (1.2 months); Dr. Koutcher directs the overall project. Funding Support – NIH

Ellen Ackerstaff ~38% - (Co-Investigator) Dr. Ackerstaff supervises all the metabolic studies performed both in vivo and in vitro. Other support – NIH

Soe Min – 50% - she takes the place of Ms. Kruchevsky and provides technical support (cell studies and in vivo studies

Paola Porcari = 50% - postdoctoral fellow; performs all the MR studies and some cell studies

Has there been a change in the active other support of the PD/PI(s) or senior/key personnel since the last reporting period?
If there is nothing significant to report during this reporting period, state "Nothing to Report."

If the active support has changed for the PD/PI(s) or senior/key personnel, then describe what the change has been. Changes may occur, for example, if a previously active grant has closed and/or if a previously pending grant is now active. Annotate this information so it is clear what has changed from the previous submission. Submission of other support information is not necessary for pending changes or for changes in the level of effort for active support reported previously. The awarding agency may require prior written approval if a change in active other support significantly impacts the effort on the project that is the subject of the project report.

See below.

KOUTCHER, JASON
New Grant Since Last Submission
W81XWH2110101 (PI: Koutcher) 9/30/2021 - 9/29/2024 1.80 calendar
Congressionally Directed Medical Research Programs
Enhancing Breast Cancer Therapy by Inhibiting the Adenosine Receptor and Oxygen Consumption
Study the effects of AZD4635 (A2aR inhibitor), DFP, and MET on tumor cell OCR and proliferation and immune cell function. Determine if a reduction of OCR enhances the efficacy of adenosine blockade.
Role: PD/PI

ACKERSTAFF, ELLEN
New Grant Since Last Submission
W81XWH2110101 (PI: Koutcher) 9/30/2021 - 9/29/2024 3.00 calendar
Congressionally Directed Medical Research Programs
Enhancing Breast Cancer Therapy by Inhibiting the Adenosine Receptor and Oxygen Consumption
Study the effects of AZD4635 (A2aR inhibitor), DFP, and MET on tumor cell OCR and proliferation and immune cell function. Determine if a reduction of OCR enhances the efficacy of adenosine blockade.
Role: Co-Investigator

What other organizations were involved as partners?
If there is nothing significant to report during this reporting period, state "Nothing to Report."

Describe partner organizations – academic institutions, other nonprofits, industrial or commercial firms, state or local governments, schools or school systems, or other organizations (foreign or domestic) – that were involved with the project. Partner organizations may have provided financial or in-kind support, supplied facilities or equipment, collaborated in the research, exchanged personnel, or otherwise contributed.

None.

8. SPECIAL REPORTING REQUIREMENTS

COLLABORATIVE AWARDS:

Partnering PI award (W81XWH-17-1-0526) ended September 14, 2021 and thus an independent final report will be submitted in January 2022. No annual technical report will be provided.

QUAD CHARTS: *Not applicable.*

9. APPENDICES: *Attach all appendices that contain information that supplements, clarifies or supports the text. Examples include original copies of journal articles, reprints of manuscripts and abstracts, a curriculum vitae, patent applications, study questionnaires, and surveys, etc.*